# Marshall Plan Scholarship
# Final Research Paper

by

Caroline SCHÄTZ

# GENERATION OF LIVING BLOOD VESSELS FROM HYPOIMMUNOGENIC HUMAN PLURIPOTENT STEM CELLS

**Internal Supervisor**: Doris Ripper, PhD
**External Supervisor**: Torsten Meissner, PhD

Submitted on: 25.02.2020

# Declaration of Honor

*“I declare on my word of honor that I have written this paper on my own and that I have not used any sources or resources other than stated and that I have marked those passages and/or ideas that were either verbally or textually extracted from sources. This also applies to drawings, sketches, graphic representations as well as to sources from the internet.*
*The paper has not been submitted in this or similar form for assessment at any other domestic or foreign post-secondary educational institution and has not been published elsewhere. The present paper complies with the version submitted electronically.”*

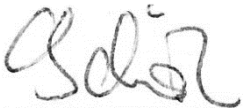

***Date:*** *25.02.2020* ***Signature***

## Acknowledgements

Firstly, I want to express my gratitude to the Marshall Plan Foundation for the greatly appreciated financial support.

My next words of thank go to my external supervisor at the Beth Israel Deaconess Medical Center, one of the Harvard Medical School teaching hospitals, Torsten Meissner. Thank you for your advice and will to share your knowledge with me. My sincere gratitude for encouraging and supporting me during my time in Boston.

Also, I would like to express my gratefulness to my internal supervisor Dr. Doris Ripper for always having an open ear for my questions. Many thanks go to the whole team of my home university, especially Dr. Barbara Entler for her organizational support and of course our program director Dr. Harald Hundsberger.

Moreover, I would like to thank my colleagues in the Chaikof, Cowan and Strominger labs who introduced me to their world of science, always supported me when needed and also showed me some of the best places Boston has to offer. It was an honor being part of such international, interdisciplinary and great groups.

Last but not least, I would like to say thank you to my family and dearest friends who supported me during my whole internship, be it financially or also mentally. Thank you for always being there and encouraging me.

# Abstract

For the treatment of cardiovascular disease there is a need for vascular grafts to substitute affected human blood vessels. To generate tissue-engineered vascular grafts, a novel protocol was developed where vascular wall cells are seeded onto collagen sheets and rolled around a mandrel. For this thesis, the focus was on the preparation of the cellular building blocks, from which two major research questions arose. The first one was if it is possible to differentiate the human induced pluripotent stem cell (hiPSC) line #86 and the genome-edited hypoimmunogenic #86 B2M$^{-/-}$/CIITA$^{-/-}$ into endothelial (ECs) and vascular smooth muscle cells (VSMCs). Following, the correlation of the hiPSC-derived ECs and VSMCs with their primary counterparts was analyzed. As a result, it was possible to successfully differentiate the hiPSC line #86 as well as the genome-edited #86 B2M$^{-/-}$/CIITA$^{-/-}$ into ECs and VSMCs. The phenotype of the cells was characterized by flow cytometry and immunocytochemistry, using certain cell-type specific markers. The functionality of the ECs was tested and no further differences between the primary, the wildtype #86 and the genome-edited #86 B2M$^{-/-}$/CIITA$^{-/-}$ cell lines could be observed when performing a tube formation assay, TNFα-induced ICAM-1 upregulation or cellular Ox-LDL uptake. For the maturation of the VSMCs to a rather contractile phenotype, three different approaches were tested and compared. RepSox treatment in the first and second maturation approach showed some promising MYH11 upregulation. Further experiments are needed to clarify if it is applicable to all used cell lines. Torin-1 treatment increased MYH11 expression in one out of three tested cell lines. Additional work needs to be done by testing if the hPSC-derived vascular wall cells have the ability to stick to the collagen sheets used for fabricating the tissue-engineered vascular grafts. Finally, the vascular graft needs to be tested *in vivo* for maintenance of phenotypic stability as well as evasion of immunological rejection.

# Table of Contents

# List of Figures

# List of Tables

# List of Abbreviations

| | |
|---|---|
| AoSMCs | aortic smooth muscle cells |
| αSMA | α-smooth muscle actin |
| B2M | β2-microglobulin |
| COL1A1 | collagen type I alpha I |
| ECs | endothelial cells |
| ECM | extracellular matrix |
| ePTFE | expanded polytetrafluoroethylene |
| ESCs | embryonic stem cells |
| FACS | fluorescence-activated cell sorting |
| FBS | fetal bovine serum |
| HLA | human leukocyte antigen |
| hPSCs | human pluripotent stem cells |
| HUVECs | human umbilical vein endothelial cells |
| ICAM-1 | intercellular adhesion molecule 1; CD54 |
| iPSCs | induced pluripotent stem cells |
| IF | immunofluorescence |
| LFA-1 | lymphocyte function-associated antigen 1 |
| MACS | magnetic-activated cell sorting |
| MYH11 | smooth muscle myosin heavy chain; SMMHC |
| OxLDL | oxidized LDL |
| PAF | platelet activating factor |
| PBS | phosphate buffered saline |
| PDGF | platelet-derived growth factor |
| PDGFRB | platelet derived growth factor receptor beta; CD140b |
| PECAM-1 | platelet endothelial cell adhesion molecule 1; CD31 |
| PFA | paraformaldehyde |
| PMBCs | human peripheral blood mononuclear cells |
| SFM | serum free medium |
| SM22α | transgelin |
| VE-cadherin | vascular endothelial cadherin; CD144 |
| VEGFR2 | vascular endothelial growth factor 2; KDR |

| | |
|---|---|
| VSMCs | vascular smooth muscle cells |
| vWF | von Willebrand’s factor |
| WT | wildtype |

# 1 Introduction

## 1.1 Vascular Disease

To date, there are many restraints in treatment of cardiovascular diseases, even though they are one of the most common diseases in the Western population. Atherosclerosis, which describes the process occlusion of the blood vessel due to deposition of plaques, can lead to peripheral or coronary artery disease. If untreated, such events happen to end with loss of a limb, heart attack or stroke (Topol, 2007).

Treatment of cardiovascular diseases remains still restricted. There are various approaches depending on the certain type of vascular disease and where the occluded or unfunctional vessel is located in the body. In case of a blood vessel occlusion through an upbuilding plaque, which consists mainly out of deposits of fat and cholesterol, there is a possibility to remove the plaque surgically. Removal is necessary, as otherwise the plaque could either completely occlude the blood vessel leading to loss of blood circulation in the corresponding region or the plaque could loosen from the cell wall and travel with the blood flow to the coronary arteries, where blockage can ultimately lead to a heart attack. Usually, the first surgical approach to remove the plaque would be to perform an angioplasty. If necessary, a stent can be placed to keep the blood vessel open. However, if the diseased blood vessel is already too damaged to be cleared by angioplasty and a stent implant, the conventional surgical procedure is placing a bypass around the occluded vessel so that blood flow can be maintained, and symptoms of the patient are reduced. It is important to mention that a bypass surgery is no definite cure of the arterial disease, it just eases the patient's symptoms for a limited amount of time (National Heart, 2006; Topol, 2007).

However, various problems arise when performing a bypass surgery. Firstly, people in need of a bypass surgery usually are not in superior medical conditions. This means that autologous blood vessels taken from them for their bypass are already in unfavorable conditions which could lead to decreased levels of patency or early relapse in the following years. Moreover, there is a limited number of vessels

that can be taken out of a body and used at different sites for bypassing a clotted vessel. Because of these reasons amongst others, various researchers have been trying to develop vascular grafts for use in prosthetic bypass surgery for many years (Mehta et al., 2011).

Currently, success of clinical transplantation of solid organs is more the result of advances in immunosuppressive therapy. This is due to the fact that overcoming the immune barrier is a major obstacle in engineering living tissues for transplantation. The incompatibility and immune rejection of foreign grafts are for the most part based on the highly polymorphic human leukocyte antigens (HLA), of which so far more than 17,000 different alleles are identified in the human population (Conte et al., 2006). All these reasons just underline the pressing need of a functional vascular graft that has clinical relevance. This is why this project aims at producing immunoevasive living blood vessels that can be used for any patient as off-the-shelve products.

## 1.2 Human Pluripotent Stem Cells

Stem cells are unspecialized cells of the human body that possess the ability to differentiate into all somatic cell types. In 1998, the first embryonic stem cells (ESCs) were isolated by James A. Thomson (Thomson et al., 1998). ESCs are pluripotent cells, meaning that they can differentiate into all three germ layers (endoderm, mesoderm and ectoderm) but not into extraembryonic structures such as the placenta. However, as ESCs are isolated from the inner cell mass of a blastocyst, which constitutively forms the embryo, the usage of ESCs is ethically debatable (Zakrzewski, Dobrzynski, Szymonowicz, & Rybak, 2019).

In 2006, Takahashi and Yamanaka identified four factors (Oct4, Sox2, Klf4 and cMyc) with which it became possible to reprogram fully differentiated cells into pluripotent stem cells, which were then called induced pluripotent stem cells (iPSCs) (Takahashi & Yamanaka, 2006). This discovery set a starting point for a new field in stem cell regenerative therapy where iPSC lines can be produced in a customized and biocompatible manner (Zakrzewski et al., 2019).

### 1.2.1 Generation of Universal Donor Stem Cells

Generation of autologous iPSC makes use of reprogramming the patient's own somatic cells that can be obtained from various adult tissues. However, generation of such autologous stem cells takes time, usually three to four weeks, and so far, has very low efficiency (Mattapally et al., 2018). For clinical applications of stem cell therapies there is a search for the ultimate universal donor cell which can be used for any cell therapy purpose without evoking an immune rejection due to HLA mismatching (Han et al., 2019).

There exist various approaches on how to render cells immunoevasive. In this project hypoimmunogenic stem cells were created by using CRISPR/Cas9 to knock out HLA class I and II. HLA class I expression was knocked out by targeting β2-microglobulin (B2M) which is needed for proper antigen presentation of HLA class I. HLA class II expression was ablated by targeting the CIITA gene, which functions as a master regulator of HLA class II. The structure of HLA class I and II can be seen below in Figure 1.

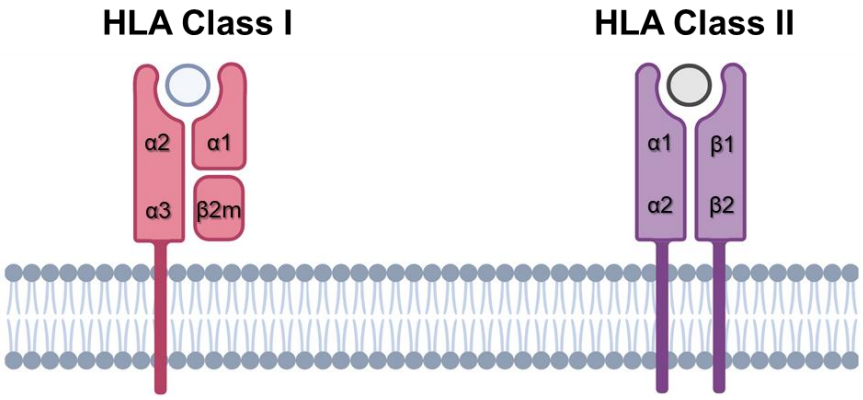


***Figure 1**: Structure of HLA class I and II heterodimeric transmembrane proteins. HLA class I consists of a heavy chain with three globular domains (α1, α2, and α3) and is non-covalently bound to β2m. HLA class II is made up of two heavy chains (α-chain and β-chain) each with two globular domains (α1 and α2 or β1 and β2). The α1 and α2 domains of HLA class I, and the α1 and β1 domains of HLA class II, form the peptide-binding groove. (The image was created with BioRender.com.)*

## 1.3 Differentiation of Cells

Differentiation of human pluripotent stem cells (hPSCs) represents maturation processes occurring during embryonic development. In 1957, Conrad Waddington proposed in his publications a simplified metaphorical representation of how decisions on cell differentiation and cell fate are made, nowadays referred to as the Waddington diagram (Waddington, 1957), a modified version is shown in Figure 2. Basically, it demonstrates how a totipotent stem cell starts its development by undergoing a series of successive branching lineage decisions, stepwise ending up more differentiated and mature. Cellular identity shifts from totipotency to pluripotency, multipotency and ultimately to terminal unipotency (Rajagopal & Stanger, 2016).

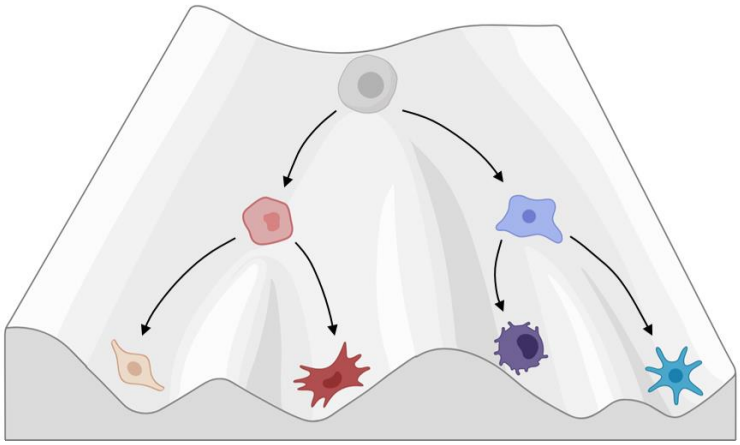

***Figure 2**: Modified version of the Waddington diagram showing the cellular lineage decisions. They represent the differentiation from a totipotent or pluripotent stem cell to more specialized multipotent or unipotent cells. (The image was created with BioRender.com.)*

If having hPSCs as a starting point, the first step of differentiation is a lineage decision. In humans there exist three lineages out of which eventually the whole organism develops, namely endoderm, mesoderm and ectoderm (G. Wu & Scholer, 2016). Blood and associated organs, such as blood vessels, originate from the mesoderm lineage (Loh et al., 2016). In this project, after induction of a mesodermal fate of the cells, certain growth factors are added to induce specification of the cells into

endothelial cells (ECs) and vascular smooth muscle cells (VSMCs) (Patsch et al., 2015; Zhang et al., 2019).

### 1.3.1 Endothelial Cells

ECs cover the whole human vasculature as a monolayer in the vessel lumen, forming an interface between the circulating blood and the outer layers of the blood vessel. To comply with their semipermeable barrier function, ECs establish sealing adherent and tight junctions. As already mentioned, ECs are derived from the lateral plate mesoderm (Mazurek et al., 2017). During embryogenesis arterial and venous fate of ECs appears to be initially regulated on the transcriptional level and molecular pathways including molecules such as Hedgehog, VEGF and Notch. However, arteriovenous specification is further sustained by blood flow forces (Fang & Hirschi, 2019; Qiu & Hirschi, 2019). ECs play an important role in angiogenesis as they enable a dynamic progression of vessel formation by migration of extruding cells with filopodia and following stalk cells. Moreover, they are involved in coagulation and inflammation processes as well as in blood flow regulation. They produce several important molecules which control blood vessel function, amongst them platelet-derived growth factor (PDGF), von Willebrand's factor (vWF) and platelet activating factor (PAF) (Tennant & McGeachie, 1990). Due to their important role in vascular homeostasis EC dysfunction can lead to several pathological disorders (Mazurek et al., 2017).

### 1.3.2 Vascular Smooth Muscle Cells

VSMCs are responsible for the regulation of the vascular blood flow by adjusting the vessel diameter by contraction and relaxation of the cells. The contractile state can be achieved as VSMC contain several contractile and cytoskeletal proteins, as for example α-smooth muscle actin (αSMA), transgelin (also SM22α) or smooth muscle myosin heavy chain (SMMHC, MYH11). Depending on the site of the blood vessel, or even within different regions of the same blood vessel, different types of VSMCs exist. There is either a fully differentiated contractile phenotype or

a rather migratory and proliferative synthetic phenotype (Mazurek et al., 2017). Synthetic phenotype is associated with stenosis in vascular disease and transplants (Zhang et al., 2019). Hence, a rather contractile phenotype is desired as an outcome of the differentiations performed in this thesis.

## 1.4 Tissue – Engineering of Blood Vessels

Human blood vessels are structured in three defined layers: the tunica intima, tunica media and tunica adventitia. The tunica intima forms the inner layer of the vessel and consists out of an EC monolayer which lines to vascular lumen. VSMCs are common in the vascular middle layer, or tunica media. However, there are differences in thickness as generally veins have a thinner tunica media than arteries. The outer layer, the tunica adventitia, is comprised of fibroblasts, progenitor cells and extracellular matrix (ECM) (Mazurek et al., 2017).

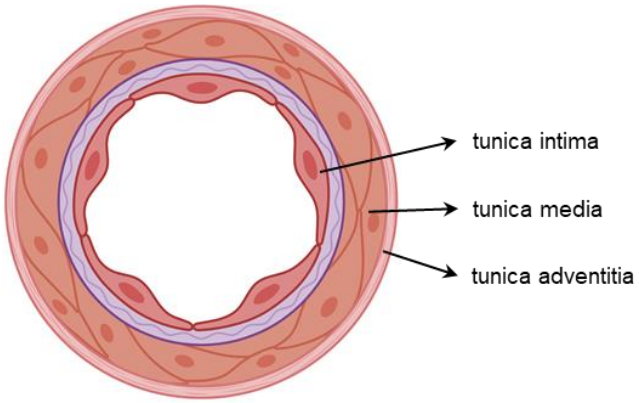


***Figure 3**: Structure of a human blood vessel. It is structured in three layers: the tunica intima (endothelial cells), the tunica media (majorly vascular smooth muscle cells and collagen) and the tunica adventitia (extracellular matrix, progenitor and fibroblast-like cells). (The image was created with BioRender.com.)*

Several approaches have been developed in the pursuit of finding suitable vascular grafts enabling clinical usage. To mimic the characteristics of arterial cell walls and to find other ways how to treat cardiovascular diseases, alternative forms of therapy have been developed, such as using synthetic scaffolds (e.g. expanded polytetrafluoroethylene (ePTFE)) as a replacement for occluded blood vessels (Roh

et al., 2008). Already more developed approaches try to incorporate resident vascular cell types to biodegradable scaffolds to promote *in situ* regeneration of the blood vessel and to ensure better compliance and patency after implantation (Roh et al., 2010). Another method that was tested by certain research groups, was to seed vascular wall cells on a biodegradable scaffold, maturate the graft within a bioreactor and then implant it into the living cardiovascular system (Dahl et al., 2011).

Ultimately there were also some approaches that exclusively made use of human cultured vascular cells, such as ECs, VSMCs or fibroblasts without any synthetic scaffold (L'Heureux et al., 2006; L'Heureux, Paquet, Labbe, Germain, & Auger, 1998). In this research project the way of producing a tissue engineered blood vessel falls into this category. A schematic illustration of the project strategy can be seen in Figure 4.

Nonetheless, limitations exist for each approach, either a too long waiting time (e.g. 3-6 months for seeding a biodegradable scaffold), the need for complex processes like decellularization to avoid allogeneic immune responses, the risk of inadequate regeneration of circulating stem cells within a biodegradable scaffold or the lack of resembling the composition and microstructure of a native vessel wall in a tolerable manner. Moreover, practical means do not exist for rapid and scalable production of patient specific vascular wall cells yet (Quint et al., 2011; Syedain, Meier, Bjork, Lee, & Tranquillo, 2011; W. Wu, Allen, & Wang, 2012).

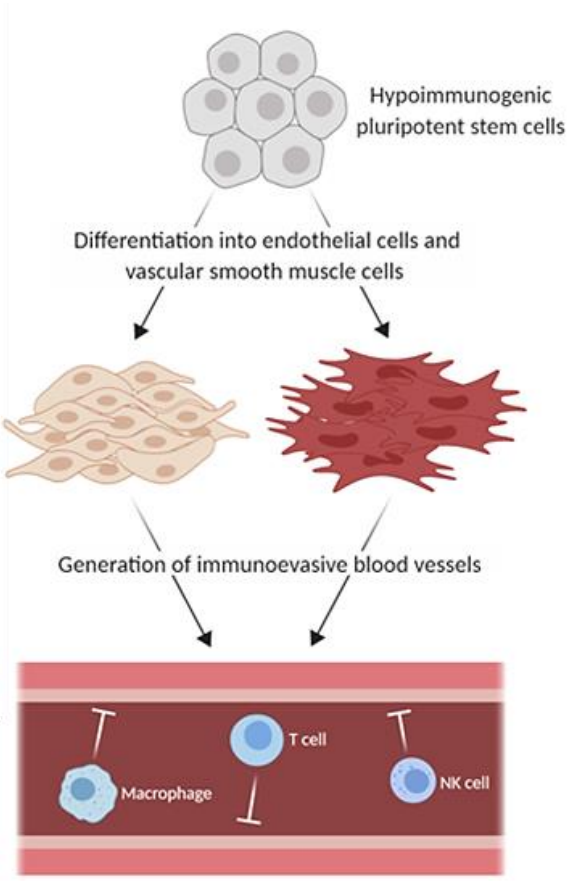


***Figure 4**: Graphical abstract of project strategy.(The image was created with BioRender.com.)*

## 1.5 Research Questions

For this project, three major research questions were defined. For generating living blood vessels, the cellular building blocks were to be produced. The first aim was to learn and optimize the technique of differentiating hPSCs into ECs and VSMCs, as these two are the prevalent cell types present in blood vessels. The second aim was to test if a specific hiPSC-line, which was named #86, could be used for the differentiation into ECs and VSMCs. Next to the wildtype #86 hiPSC-line, there was also a genome-edited #86 cell line, which was rendered to be hypoimmunogenic. It should be checked if there were any differences regarding the differentiation efficiencies and cellular identity. Finally, as a third aim, the fully differentiated cells should be characterized regarding their phenotype and their functionality.

Figure 5 below shows the schematic illustrations of the differentiation strategies for ECs (Figure 5A) and VSMCs. For the VSMC differentiation two different strategies were compared (Figure 5B and C).

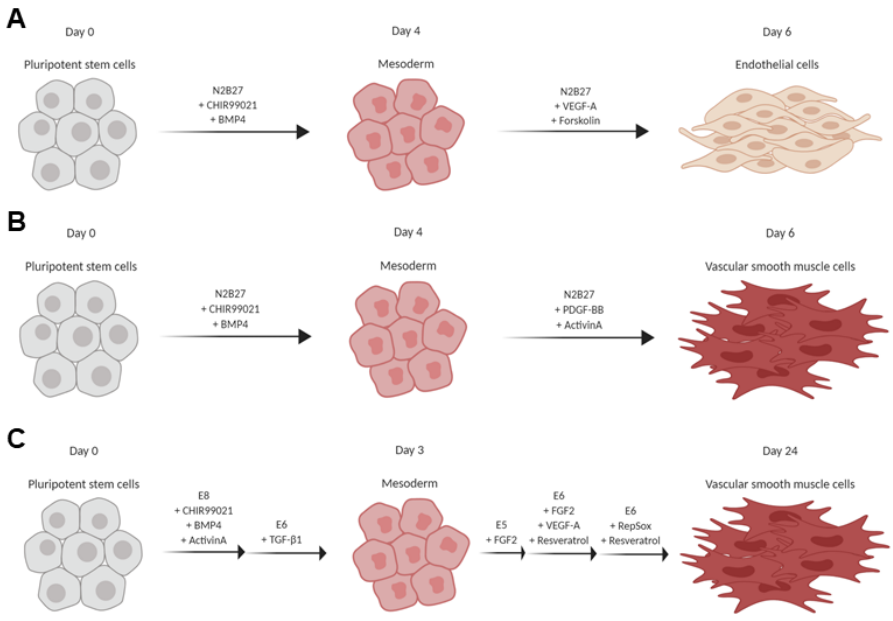


***Figure 5**: Schematic illustration of differentiation strategies. **A** Endothelial cell differentiation strategy. **B** Vascular smooth muscle cell differentiation strategy 1. **C** Vascular smooth muscle cell differentiation strategy 2. (The images were created with BioRender.com.)*

For the induction of the contractile phenotype of VSMCs, two different molecules were tested for their ability to maturate the cells: RepSox and Torin-1. RepSox promotes the NOTCH signaling pathway and was thus found to enhance cellular contractility (Zhang et al., 2019) whilst Torin-1 is an inhibitor of mTOR (mTORC1 and mTORC2) which was previously used for maturating cardiomyocytes (Garbern et al., 2019).

In a bigger picture, the cells which were created during this project are to be used for generating hypoimmunogenic living blood vessels in the future. A microfluidic bioprinter is to be used to produce collagen sheets on which the hypoimmunogenic hiPSC-derived VSMCs are seeded. After an incubation period, the seeded collagen sheets are rolled around a mandrel to create a tube-like structure. Finally, hypoimmunogenic iPSC-derived ECs are seeded in the lumen of the graft to resemble the tunica intima, the inner lining of the blood vessel. However, the focus of this research project is the generation of the cellular building blocks for the tissue-engineering of vascular grafts.

# 2 Materials & Methods

## 2.1 hPSC Culture and Differentiation

Cells were maintained at 37°C in a humidified incubator containing 5% $CO_2$. The used hiPSC line in this bachelor thesis is called #86 (Panopoulos et al., 2017), which was initially reprogrammed from fibroblasts. As a differentiation control the human embryonic stem cell (ESC) line H9 was chosen (Thomson et al., 1998). The hPSCs were maintained in Geltrex-coated (Gibco, A14132-02) culture dishes in either mTeSR-1 (StemCell Technologies, 85850) or StemFit Basic02 (Ajinomoto) medium. Cells were routinely passaged before they reach confluence using Accutase (Corning, 25058CI) at dilutions of 1:6 to 1:12. They were seeded into medium containing 10µM ROCK inhibitor Y-27632 (ChemCruz, SC-281642A). Stocks of hPSCs were made using mFreSR (StemCell Technologies, 05855) as freezing medium.

For differentiations 1.5 x $10^6$ cells were plated per 10 cm culture dish. **EC differentiation** was started by changing the medium after 24 h to medium 1 consisting of N2B27 medium (1:1 mixture of DMEM/F12 and neurobasal medium with N2 and B27 supplements [both Thermo Fisher Scientific]) with 6 µM CHIR and 25 ng/mL BMP4. After 3 days, medium 2 was used, consisting of N2B27 supplemented with 20 ng/mL VEGF and 2 µM forskolin. On day 6, the ECs were either purified using magnetic-activated cell sorting (MACS) with CD144 magnetic beads or stained for CD144 and subsequently sorted. They were plated on fibronectin coated culture dishes and then fed every other day with EC maintenance medium and passaged using 0.05% Trypsin (Corning, 25-051-CI) and DMEM (Corning, 10-017-CV) + 10% FBS (Hyclone, SH30071.02). For expansion different media were tested – either EGM-2 MV EC medium (EBM-2 [Lonza, CC-3156] supplemented with EGM-2 MV SingleQuots [Lonza, CC-4147]), E7V medium (E6 medium [Thermo Fisher, A1516401] supplemented with 100 ng/mL FGF2 and 50 ng/mL VEGFA as used in a protocol developed by (Zhang et al., 2017) or serum-free medium [Gibco, 11111-044] supplemented with 20 ng/mL FGF2 and 50 ng/mL VEGFA (in the following abbreviated with SFM).

Two different protocols were used for the **VSMC differentiation**. Strategy 1, according to Patsch *et al.* (2015), started in the same way as the EC differentiation. 1.5 x $10^6$ cells were seeded in a coated 10 cm culture dish. From day 1-3, N2B27 medium was supplemented with 6 µM CHIR and 25 ng/mL BMP4. On day 4 and 5, the cells were fed with N2B27 medium supplemented with 10 ng/mL PDGF-BB and 2 ng/mL Activin A. Finally, the cells were replated in VSMC maintenance medium (DMEM mixed with SmGM-2 SingleQuots [Lonza, CC-4149]) on day 6 at a density of 3.5 x $10^4$ cells/$cm^2$. They were subsequently fed every other day with SmGM-2 VSMC maintenance medium and passaged using 0.25% Trypsin and DMEM + 10% FBS.

Strategy 2 of the VSMC differentiation was performed according to a protocol developed in the University of Madison-Wisconsin by Zhang *et al.* (2019). On day 0, the cells were plated in a Geltrex-coated culture dish at a density of 1 x $10^5$ cells/$cm^2$ into E8BAC medium (E6 medium with 100 ng/mL FGF2, 2 ng/mL TGF-β, 5 ng/mL BMP4, 25 ng/mL Activin A and 1 µM CHIR). After 36 h, the cells were passaged and seeded onto a new Geltrex-coated plate at a density of 1-4 x $10^4$ cells/$cm^2$ in E6T medium (E6 medium with 1.7 ng/mL TGF-β). After 18 h, the medium was replaced with E5F medium (E5 medium [Stemcell Technologies, 05916] with 100 ng/mL FGF2). This medium was used for 6 days, until day 8. Then, FVR medium (E6 medium with 100 ng/mL FGF2, 50 ng/mL VEGFA and 25 µM Resveratrol) was used for four days, from day 9-12. For maturation E6R (E6 medium with 25 µM Resveratrol and 25 µM RepSox) medium was used for 12 more days, from day 13-24. On day 16 however, the cells were split at a density of 1 x $10^5$ cells/$cm^2$. Medium was usually exchanged every other day if not specifically indicated otherwise. Samples for FACS analysis and RNA were harvested on days 16 and 24. The differentiated VSMC were maintained either in SmGM-2 VSMC medium or in E6R medium.

Primary cell lines used as controls were human umbilical vein endothelial cells (HUVECs; Lonza, CC-2517) and aortic smooth muscle cells (AoSMCs; Lonza, CC-2571). Stocks of ECs and VSMCs were made using CryoSFM (PromoCell, C-29912) as a freezing medium.

## 2.2 Magnetic-Activated Cell Sorting

MACS purification was performed according to the manufacturer's instructions (MACS Miltenyi Biotec). Cells were harvested and a cell count was received. Then, the cells were pelleted at 1600 rpm for 5 min. The supernatant was aspirated, and the pellet got resuspended in 80 µL MACS buffer per $10^7$ cells. 20 µL of CD144 microbeads per $10^7$ cells were added and mixed well. The cells were incubated in the refrigerator for 15 min. After that, the cells were washed twice with 2 mL of MACS buffer and centrifuged at 1600 rpm for 5 min. The pellet, up to $10^8$ cells, got resuspended in 500 µL MACS buffer and filtered to a nylon mesh to remove cell clumps. For magnetic separation a LS column was placed in an appropriate magnetic stand and calibrated by rinsing with 3 mL buffer. Then, the cell suspension was applied to the column and rinsed three times with 3 mL buffer. Finally, the column was removed from the magnetic field and 5 mL buffer were added and firmly squeezed into a capture tube. The cells were pelleted again and then plated into appropriate EC medium in fibronectin-coated 10 cm cell culture dishes.

## 2.3 Cell Sorting

For cell sorting, which was performed after the EC differentiation to purify the endothelial population, the cells were harvested and pelleted. The cells were subsequently resuspended in 400 µL blocking buffer (4% FBS in PBS; pH ~7.4) for 45 min on ice. Then, 30 µL of CD144 antibody were added and the cells were incubated light-protected for 1 h on ice. After two washing steps with 3 mL of 1% FBS in PBS, the cells were resuspended in 750 µL 1% FBS in PBS. The cells were sorted into capture tubes filled with 500 µL of corresponding endothelial maintenance medium.

## 2.4 Flow Cytometry

Around 5 x $10^5$ cells were harvested and pelleted. The cells were subsequently resuspended in 200 µL blocking buffer (4% FBS in PBS) for 45 min on ice. Then, the corresponding antibody was added, usually in a 1/100 dilution, and the cells were incubated light-protected for 1 h on ice. After two washing steps with 750 µL of 1%

FBS in PBS, the cells were fixed in 300 µL of 1% paraformaldehyde (PFA). When fixed, the cells could be stored until used in flow cytometry with the CytoFLEX flow cytometer (Beckman Coulter). The used antibodies can be found in the Annex, Table 2.

## 2.5 Immunocytochemistry

For immunofluorescence (IF) staining 1.5 x $10^5$ cells were seeded per 12-well. On the next day, the cells were washed with PBS. Then, a 10-minute fixation step followed with 500 µL of 4% PFA in PBS. The cells were then blocked for 45 min with 500 µL of 10% normal donkey serum [Jackson Immuno Research, 017000121] in PBS as well as 0.1% Triton-X when staining for an intracellular antigen. Following that, there was an overnight incubation with the primary antibody at 4°C in 500 µL 5% normal donkey serum in PBS. On the next day, the cells were washed 3 times with PBS, 5 min each. Then, the cells were incubated for 45 min at RT with their corresponding secondary antibody in 1% normal donkey serum in PBS (1 µL of secondary antibody in 500 µL 1% donkey serum). Further, washing of the cells was performed 2 times and a subsequent staining with DAPI for 5 min at RT (1 µL DAPI in 10 000 µL PBS). Then, the cells were washed 2 more times and 500 µL of PBS were added. Images were acquired using a fluorescence microscope (Nikon Eclipse Ti-S, NIS-Elements BR imaging software) and analyzed using the ImageJ software. For all incubation and washing steps an orbital shaker was used. The used antibodies can be found in the Annex, Table 1.

## 2.6 Real-Time PCR

After RNA isolation with the PureLink RNA Mini Kit (Invitrogen, 12183025), 16 µL of RNA (between 1-5 µg) were mixed with 4 µL of Maxima™ H Minus cDNA Synthesis Master Mix (Thermo Fisher Scientific, M1662) for obtaining cDNA. The following PCR program was used: 25°C for 10 min, 50°C for 30 min and 85°C for 5 min. RNA concentration was measured by using the NanoDrop spectrophotometer ND-1000.

For real-time PCR (= qPCR) a Master Mix was prepared first. 5 µL of TaqMan™ Gene Expression Master Mix (Applied Biosystems, 4369016) or 2x TaqMan™ Universal PCR Master Mix (Applied Biosystems, 4304437) were mixed with 2.5 µL of nuclease-free water and 0.5 µL of TaqMan probe. 2 µL of cDNA were mixed with 8 µL Master Mix. The following qPCR program was used: 50°C for 2 min, 95°C for 10 min, 95°C for 15 sec and 60°C for 1 min whereby step 3 and 4 were repeated 40 times. The used TaqMan probes are listed in the Annex, Table 3. The used machine was the ViiA 7 from Applied Biosystems. qPCR data was analyzed using the Livak method.

## 2.7 Tube Formation Assay

In a 24-well cell culture plate 200 µL of growth factor reduced, phenol red-free Matrigel (Corning, 356231) were pipetted. During a 45-minute incubation of the plate at 37°C, the used endothelial cells were dissociated from the culture plate using 0.05% Trypsin (Corning, 25-051-CI) and stopped with DMEM + 10% FBS. The cells were pelleted and gently resuspended. Then, 5 x $10^4$ cells per 24-well were seeded into Endothelial Cell Basal Medium-2 (Lonza, CC-3156) supplemented with the EGM-2 MV SingleQuots bullet kit (Lonza, CC-4147) or E7V medium, which is serum-free E6 medium supplemented with 100 ng/mL FGF and 50 ng/mL VEGF-A. The cells on Matrigel were cultured for 48 h and pictures were taken after 24 h.

## 2.8 OxLDL Uptake

To test cellular OxLDL uptake 1.5 x $10^5$ cells were plated per 24-well in 200 µL of endothelial maintenance medium. On the next day, the cells were serum starved for 12-24 h (regular medium without serum but with 0.3% BSA was used). Then, DiI-labeled OxLDL was added at a concentration of 10 µg/mL to the starvation medium. The cells were incubated for 2-4 h at 37°C. Then the cells were rinsed three times with wash buffer (0.03% BSA in PBS) and subsequently either used for FACS or immunocytochemistry.

## 2.9 Torin-1 Assay

For the Torin-1 assay 4 x $10^5$ cells were plated per 6-well, 7.5 x $10^4$ cells were plated per 24-well. The cells were treated with Torin-1 at concentrations of 200 nM, 100 nM or 50 nM. As a control 0.02% DMSO was used. SmGM-2 VSMC maintenance medium was used. The treatment was applied for nine days, the media was changed every other day. Cells plated in 6-wells were used for subsequent qPCR. Cells plated in 24-wells were used for immunocytochemistry.

## 2.10 Statistical Analysis

Flow cytometry data was analyzed using either the FlowJo or the CytExpert software. qPCR data was analyzed using the Livak method. Statistics were done utilizing Prism8 (GraphPad Software). Error bars represent the standard error of the mean (SEM).

# 3 Results

## 3.1 Differentiation of hPSCs into Endothelial Cells

For generating ECs from hPSCs, a six-day protocol, previously published from Patsch *et al.,* was used (Fig. 6A). First there is a mesoderm induction of the hPSCs by adding CHIR99021 and BMP4 to the medium. CHIR99021 is known to promote Wnt-signalling through GSK3 inhibition and BMP4 was found to induce mesoderm formation. EC specification was mediated by adding VEGF-A and forskolin to the medium. VEGF-A is a signalling protein involved in vasculogenesis and angiogenesis. Forskolin increases intracellular cAMP levels, thus activates protein kinase A which was found to lead to an increased vascular development (Patsch et al., 2015). The exact differentiation strategy is explained in *2.1 hPSC culture and differentiation*.

Figure 6B shows representative brightfield images of three different cell lines during EC differentiation: #86, which is a female, type O iPSC line; #86 B2M$^{-/-}$/CIITA$^{-/-}$, which is a genome edited cell line devoid of HLA class I and HLA class II expression and the H9 cell line, which is an ESC line that was used as a positive control as it is widely used in the field. The images were taken on day 0, 2, 4, 6 and 7 after the MACS purification using CD144 specific magnetic beads. Morphology changes can be observed as they transform from hPSCs, where relatively small cells form tight and regular colonies, to ECs, which are already enlarged, show a polygonal, cobblestone-like shape and form regular, smooth patches.

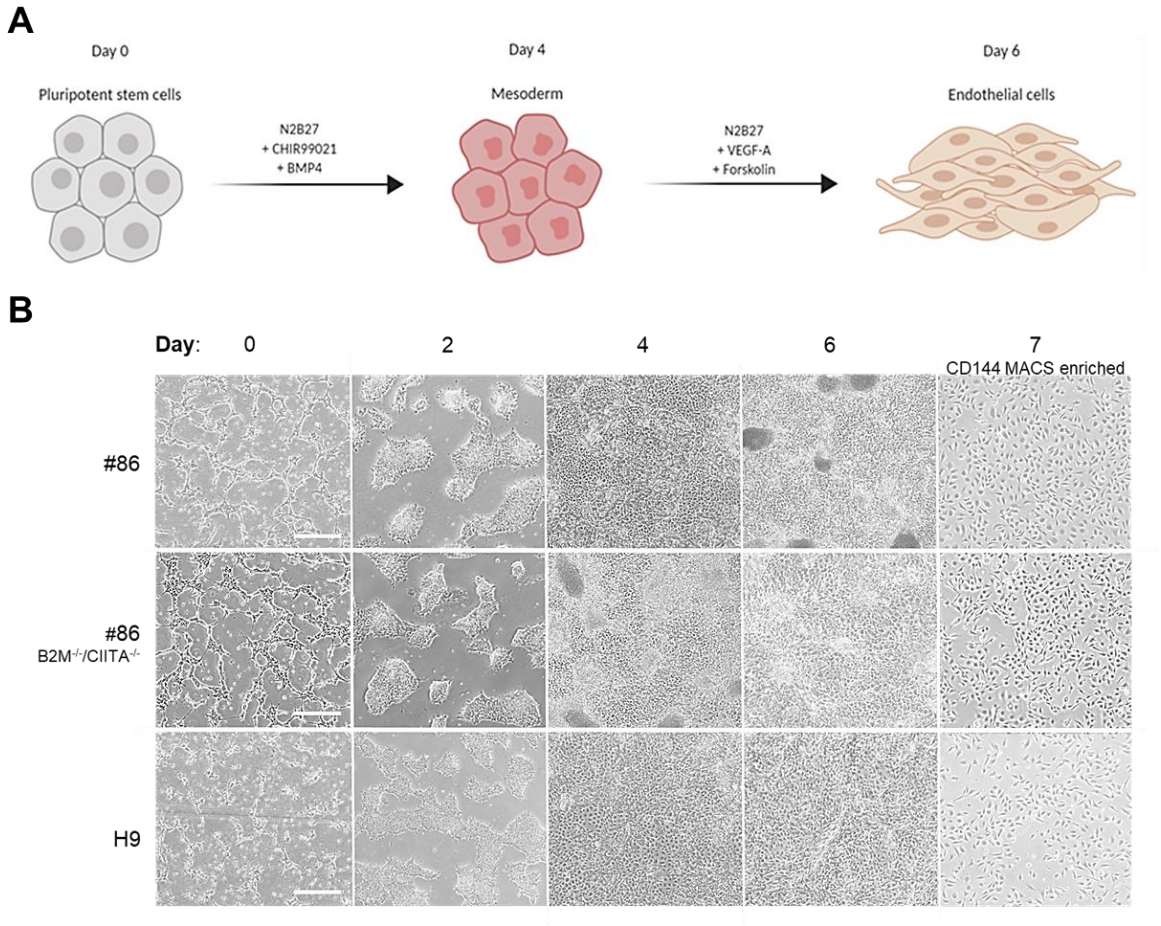


***Figure 6**: Endothelial cell differentiation. **A** Schematic illustration of the strategy for EC differentiation. (The image was created with BioRender.com.) **B** Representative brightfield images of EC differentiation of #86 and H9 on day 0, 2, 4 and 6, as well as on day 7 after MACS purification with magnetic CD144 beads. Scale bars, 200 µm.*

On day 6, an EC differentiation efficiency of 10-15% was achieved. Figure 7A shows that the genome-edited #86 cell lines, #86 B2M$^{-/-}$ and #86 B2M$^{-/-}$/CIITA$^{-/-}$, have similar differentiation efficiencies compared to the wildtype (WT) #86 iPSC- and H9 ESC-derived ECs assessed by flow cytometry. The cells were stained for CD31 which is involved in establishing intercellular junctions and is commonly used as a specific endothelial marker.

To increase the purity of the ECs, magnetic-activated cell sorting (MACS) was used. For this purification method CD144-specific antibodies coupled to magnetic beads were added to the mixed cell population containing the ECs. CD144, also named vascular endothelial cadherin (VE-cadherin), is involved in establishing intercellular

junctions, such as adherent and tight junctions. Then, the purified cells were stained for CD31, which is important for the establishment of intercellular junctions, and with fluorescence-activated cell sorting (FACS) the percentage of CD144+CD31+ could be quantified. As it can be seen in Figure 7B, the purity of the EC populations increased to around 70-80% after the MACS purification. No significant differences between the different cell lines are observed.

To obtain an entirely pure EC population, which became a necessity in further functional endothelial assays, cell sorting of CD144 stained cells was performed instead of MACS. Figure 7C shows that almost pure EC population were obtained. However, when comparing the two purification methods, MACS is a gentler way of purifying ECs. When choosing a too high flow rate for the cell sorting, a lot of cell death was observed after re-plating the cells.

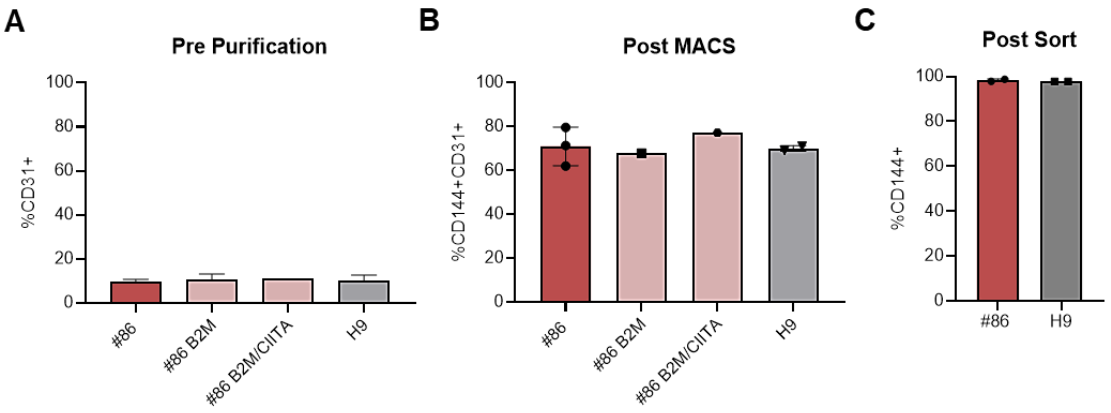


***Figure 7**: EC purity pre purification and post MACS or cell sorting, assessed by using flow cytometry. **A** Differentiation efficiency of #86, #86 B2M$^{-/-}$, #86 B2M$^{-/-}$/CIITA$^{-/-}$ and H9 ECs pre purification stained for CD31. **B** #86, #86 B2M$^{-/-}$, #86 B2M$^{-/-}$/CIITA$^{-/-}$ and H9 differentiated ECs post MACS purification using CD144 beads stained for CD31. **C** #86 and H9 differentiated ECs post cell sorting, stained for CD144.*

After having obtained a relatively pure EC population, an appropriate medium for cell expansion should be determined. Three different media and their suitability for EC culture were compared. E7V medium is serum-free E6 medium supplemented with 100 ng/mL FGF and 50 ng/mL VEGF-A. This medium was previously used in a publication of Zhang *et al*. for the culture of hPSC-derived arterial ECs (Zhang et

al., 2017). The second medium used was EBM-2 medium supplemented with the EGM-2 MV SingleQuots bullet kit, which contains FGF, EGF, VEGF, ascorbic acid, R3-IGF and hydrocortisone. Also, the medium contains 5% FBS. This medium is widely used in the field for EC culture. As a third medium serum-free medium (SFM) supplemented with 20 ng/mL FGF and 50 ng/mL VEGF was tested for expansion.

Figure 8A shows the morphology of ECs derived from #86 and H9 after six days of culture in the respective medium. The ECs for this experiment were purified by cell sorting for CD144+ cells. As all the cells died within six days in the SFM medium, this medium was not considered for further EC culture purposes. When comparing the morphology of the ECs cultured in E7V and EGM-2 MV medium, the cells seemed much more homogenous in the E7V medium. It almost looked as if the ECs in the EGM-2 MV medium possibly de-differentiated into some fibroblast-like cell type. However, when staining the cells for CD144 on day six of culture and performing flow cytometry, it was confirmed that the EC populations were still pure in both, the E7V and the EGM-2 MV medium, as can be seen in Figure 8B. Also, the cell expansion was quantified, which can be seen in Figure 8C. As the cells expanded more in the EGM-2 MV medium, this medium was chosen for further EC culture.

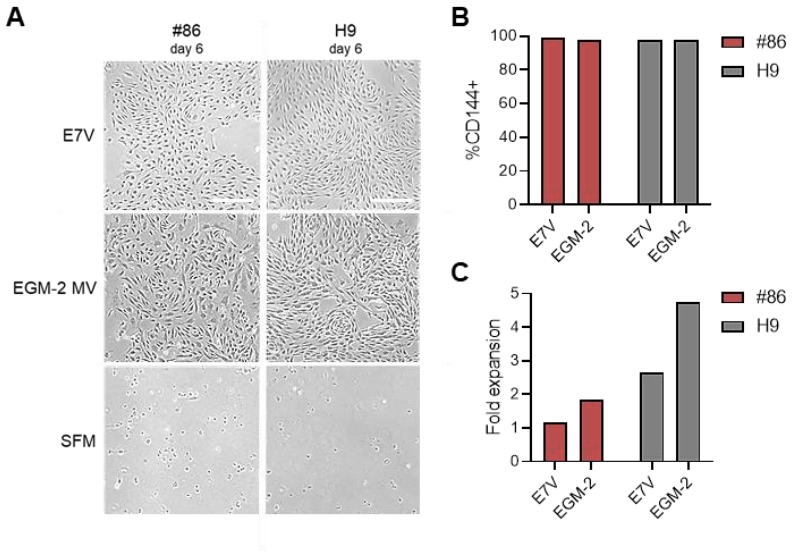


***Figure 8**: Expansion of ECs. **A** Morphology of ECs from differentiated sorted #86 and H9 after being cultured for six days in three different media: EGM-2 MV, E7V (= E6 medium supplemented with 100 ng/mL FGF and 50 ng/mL VEGFA) and SFM with 20 ng/mL FGF and 50 ng/mL VEGFA. Scale bars, 100 µm. **B** %CD144+ cells (#86 and H9 ECs) after six days of culture in above mentioned media (EGM-2 and E7V). **C** Fold expansion of ECs (#86 and H9) after six days of culture in above mentioned media (EGM-2 and E7V).*

### 3.1.1 Phenotypic Characterization

For ensuring the identity of the EC-like cells, the presence of various EC-specific cellular markers was confirmed. With immunocytochemistry the expression of vWF and CD144 could be visualized (Figure 9A). vWF is an intracellular protein involved in blood coagulation. CD144 is one of the proteins known to establish intercellular junctions. All cell lines used, HUVECs and hPSC-derived ECs from #86, #86 B2M$^{-/-}$/CIITA$^{-/-}$ and H9, show a similar pattern with CD144 at the cell membranes and vWF intracellularly expressed.

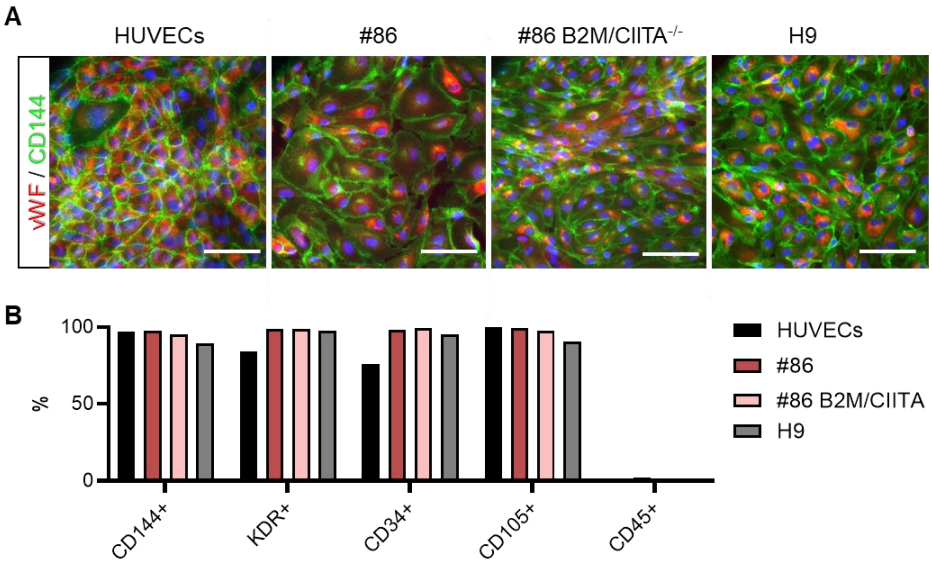


***Figure 9**: Phenotypic characterization. **A** Immunofluorescent staining of HUVECs (p6) and differentiated ECs from #86, #86 B2M$^{-/-}$/CIITA$^{-/-}$ and H9 (all p2) for vWF and CD144. Scale bars, 100 µm. **B** Characterization of primary and hPSC-differentiated EC (HUVECs, #86, #86 B2M$^{-/-}$/CIITA$^{-/-}$ and H9) by FACS with endothelial markers CD144, KDR, CD34 and CD105, gated on CD31-positive cells. CD45 was used as a negative control.*

With flow cytometry various other endothelial-specific markers were detected, which can be seen in Figure 9B. The cells were gated on CD31+ cells and then checked for CD144, KDR, CD34 and CD105 expression. CD45 was used as a negative control, as it is commonly used as an immune cell marker. CD31, also called platelet endothelial cell adhesion molecule 1 (PECAM-1), is crucial for EC junctions and

adhesion of immune cells from the blood. KDR is one of the three vascular endothelial growth factor receptors (= VEGFR2), while CD34 and CD105 are both transmembrane glycoproteins having an important role in the development of the cardiovascular system. CD45 however was found to be expressed primarily on differentiated hematopoietic cells and was thus used as a negative control. Primary HUVECs and ECs derived from the WT #86, the genome-edited #86 B2M$^{-/-}$/CIITA$^{-/-}$ and the H9 cell lines showed similar percentages of endothelial-specific marker expression. Between 80-100% of all CD31+ cells showed similar high expression for CD144, KDR, CD34 and CD105. As expected, almost no CD45+ positive cells could be detected in all used cell lines.

### 3.1.2 Functional Characterization

To test whether the hPSC-derived ECs show similar functional properties as their primary counterparts, some functional assays were performed.

The tube formation assay, as depicted in Figure 10A, demonstrated angiogenic potential of the ECs when plated on Matrigel, which served as basement membrane ECM. One of the major components of Matrigel is laminin, which is the primary factor for inducing tubule formation. It also contains certain growth factors, type IV collagen, heparan sulfate proteoglycans, entactin and nidogen (Kleinman and Martin, 2005; Kubota et al., 1988). Moreover, it contains proteases and certain other proteins. Due to its components it induces differentiation in many cell lines. Considering endothelial cells, it is known that they form capillary-like structures within 6-12 hours when seeded on Matrigel (Kleinman and Martin, 2005). When performing the assay, it could be shown that the #86, #86 B2M$^{-/-}$/CIITA$^{-/-}$ and the H9 hPSC-derived ECs possessed the ability to organize in tube-like structures. HUVECs were used as a positive control. Primary AoSMCs were used as a negative control as they were shown to inhibit tube formation when co-cultured with HUVECs in previous experiments (data not shown).

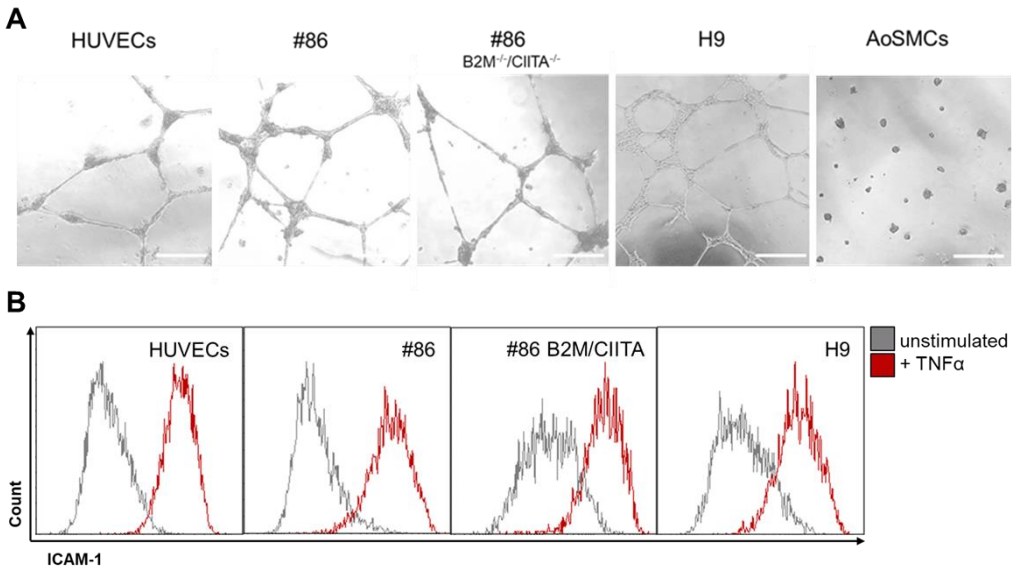


***Figure 10**: Functional characterization. **A** Tube formation assay with #86, #86 B2M$^{-/-}$/CIITA$^{-/-}$, H9 ECs post MACS with CD144 magnetic beads, HUVECs and AoSMCs. Images were taken after 24 h of seeding. Scale bars, 500 µm. **B** ICAM-1 upregulation of HUVECs (p5), #86, #86 B2M$^{-/-}$/CIITA$^{-/-}$ and H9-derived ECs (all p3) as a response to TNF-α stimulation (100 ng/mL) for 24h.*

Another well-studied functional characteristic of ECs is their tumor necrosis factor α-induced (TNFα) intercellular adhesion molecule 1 (ICAM-1, CD54) upregulation. ICAM-1 is a cell surface protein that can be usually found on ECs and cells of the immune system. There is a continuous low expression of ICAM-1 on these specific cells. However, due to cytokine stimulation, e.g. with TNFα, ICAM-1 expression is greatly upregulated. As ICAM-1 is a ligand of lymphocyte function-associated antigen 1 (LFA-1), which is typically found on lymphocytes, leukocytes start adhering to the ECs due to cytokine stimulation and can migrate into the surrounding tissues. Figure 10B shows that the primary HUVECs and the hPSC-derived WT and genome-edited cells lines all show a similar upregulation of ICAM-1 expression after TNFα stimulation (100 ng/mL) for 24 h, which was tested by staining the cells for ICAM-1 and subsequently performing flow cytometry. Interestingly, the ECs derived from #86 B2M$^{-/-}$/CIITA$^{-/-}$ iPSCs and H9 ESCs seem to already have a slightly elevated basal level expression of ICAM-1. This might be explained by differences in initial cell number and variation in growth rates. As ICAM-1 is involved in cell-cell adhesion, a higher cell density might lead to an increase in basal ICAM-1 expression due to additional formation of intercellular junctions.

To further confirm endothelial identity, the cellular uptake of oxidized low-density lipoprotein (OxLDL) was tested. OxLDL is naturally found in the human body and is an oxidatively modified variant of native LDL (Parthasarathy, Raghavamenon, Garelnabi, & Santanam, 2010). It is commonly taken up by vascular wall cells such as ECs, VSMCs as well as macrophages via certain scavenger receptors (Di Pietro, Formoso, & Pandolfi, 2016). In Figure 11A endothelial OxLDL uptake is visualized employing immunofluorescent imaging. The ECs were treated with 10 µg/mL Ox-LDL, which was coupled to the dye DiI. The red areas surrounding the nuclei enable OxLDL localization within the cell. As a control, untreated ECs were stained with only DAPI. Figure 11B quantifies the OxLDL uptake with flow cytometry. Concerning the histograms, a clear shift of the OxLDL treated samples compared to the un-treated samples could be seen. This showed that the iPSC-derived ECs #86 and #86 B2M$^{-/-}$/CIITA$^{-/-}$ and the ESC-derived ECs H9 were as capable of internalizing OxLDL as primary HUVECs.

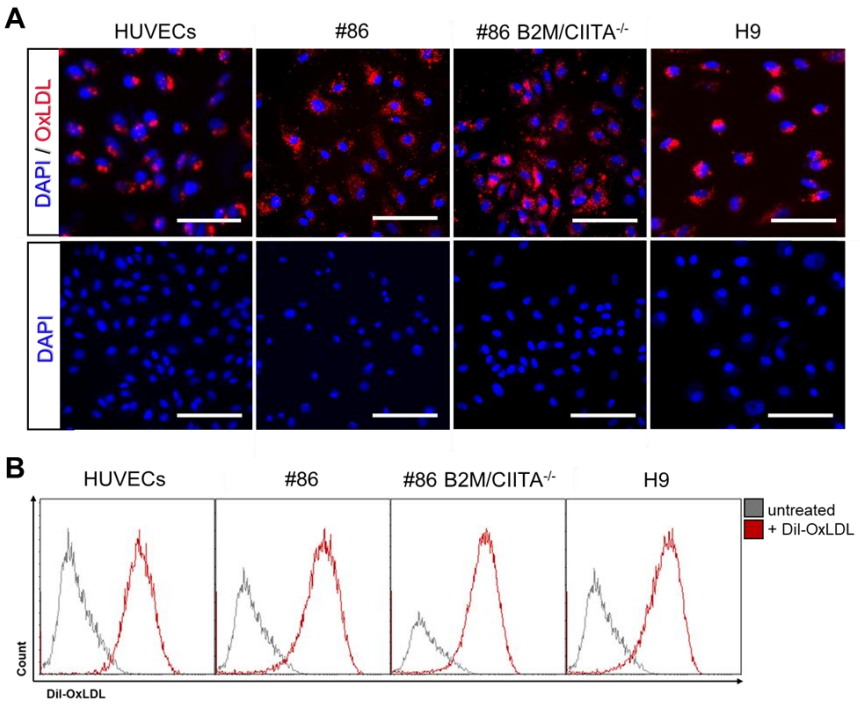


***Figure 11**: OxLDL uptake of ECs. **A** Immunofluorescence images of DiI-labelled OxLDL uptake of HUVECs, #86, #86 B2M$^{-/-}$/CIITA$^{-/-}$ and H9 post 2 h exposure at a concentration of 10 µg/mL compared to untreated controls stained only for DAPI. Scale bars, 100 µm. **B** Acquired FACS data from DiI-OxLDL treated ECs (HUVECs, #86, #86 B2M$^{-/-}$/CIITA$^{-/-}$ and H9) compared to untreated controls. Treatment occurred for 2 h at a concentration of 10 µg/mL.*

### 3.1.3 Cellular Hypoimmunogenicity

The final goal of this project is to use the iPSC-derived ECs and VSMCs in a vascular graft for clinical application. Therefore, the #86 WT iPSCs were genome-edited in order to obtain a hypoimmunogenic phenotype and to avoid immune rejection of allogeneic cells. In general, various approaches exist on how to theoretically immune-silence cells. For this project, the aim was to knock-out two major genes involved in HLA expression – B2M and CIITA. B2M is essential for proper formation of HLA class I molecules on the cell surface. Disruption of the B2M gene results thus in a lack of HLA class I expression (Wang, Quan, Yan, Morales, & Wetsel, 2015). CIITA however is a transcriptional coactivator of HLA class II. Hence, knocking out CIITA leads to absence of HLA class II expression (Masternak et al., 2000).

The histograms in Figure 12 show the iPSC-derived #86 and #86 B2M$^{-/-}$/CIITA$^{-/-}$ ECs stained for HLA class I and HLA class II. The grey curves show the unstained control while the light red histograms represent the stained samples and the dark red histograms represent the stained samples that were previously stimulated with IFNγ for 48 h at a concentration of 10 ng/mL. When comparing the #86 and #86 B2M$^{-/-}$/CIITA$^{-/-}$ cells on Figure 12A, it can be clearly seen that the #86 B2M$^{-/-}$/CIITA$^{-/-}$ cells are devoid of HLA class I expression even if stimulated with IFNγ.

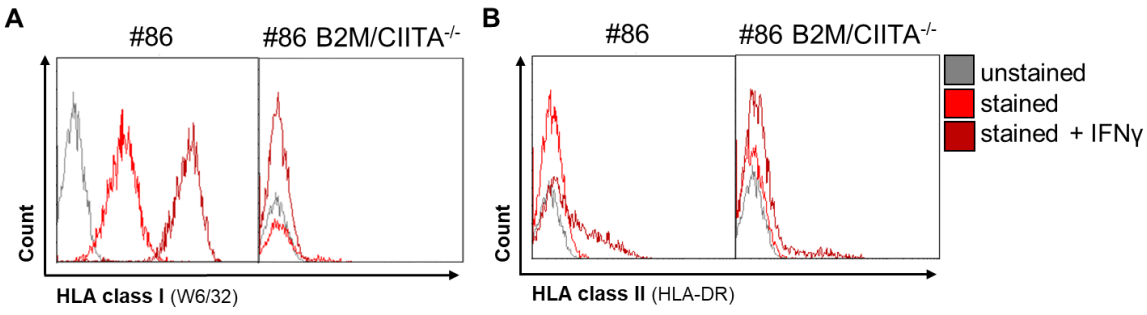


***Figure 12**: Hypoimmunogenicity of genome-edited ECs. **A** Differentiated ECs from #86 and #86 B2M$^{-/-}$/CIITA$^{-/-}$ (both p2) stained for HLA class I (W6/32 antibody) either untreated or upon IFNγ stimulation (10 ng/mL for 48 h) gated on CD31+ cells. **B** Differentiated ECs from #86 and #86 B2M$^{-/-}$/CIITA$^{-/-}$ (both p2) stained for HLA class II (HLA-DR antibody) either untreated or upon IFNγ stimulation (10 ng/mL for 48 h) gated on CD31+ cells.*

In Figure 12B #86 and #86 B2M$^{-/-}$/CIITA$^{-/-}$ cells were stained for HLA class II. No

drastic shift in HLA class II expression can be seen. However, there is a clear shoulder of the #86 IFNγ-stimulated sample, indicating HLA class II expression. In comparison, the #86 B2M$^{-/-}$/CIITA$^{-/-}$ IFNγ-stimulated sample exhibits a reduced expression of HLA class II. The residual expression could indicate either a heterozygous CIITA knock-out or a mixed population. Further confirmatory experiments or a re-targeting of the clone would be necessary.

## 3.2 Differentiation of hPSCs into Vascular Smooth Muscle Cells

### 3.2.1 VSMC Differentiation – Strategy 1

For generating VSMCs from hPSCs, two different differentiation protocols were compared. Strategy 1 correlates with the used EC differentiation protocol as it also takes six days and starts with mesoderm induction of the hPSCs and subsequent VSMC specification mediated by adding PDGF-BB and Activin-A to the medium. Both molecules were shown to stimulate VSMC formation (Owens, Kumar, & Wamhoff, 2004). It was as well previously published in Patsch *et al.* 2015. A schematic illustration of the VSMC differentiation strategy can be seen in Figure 13A. On day 6, the cells were split and further cultured in SmGM-2 medium. When split at a lower density, the cells already exhibit an elongated and stretched-out phenotype, which is typical for VSMC, which can be seen in Figure 13B.

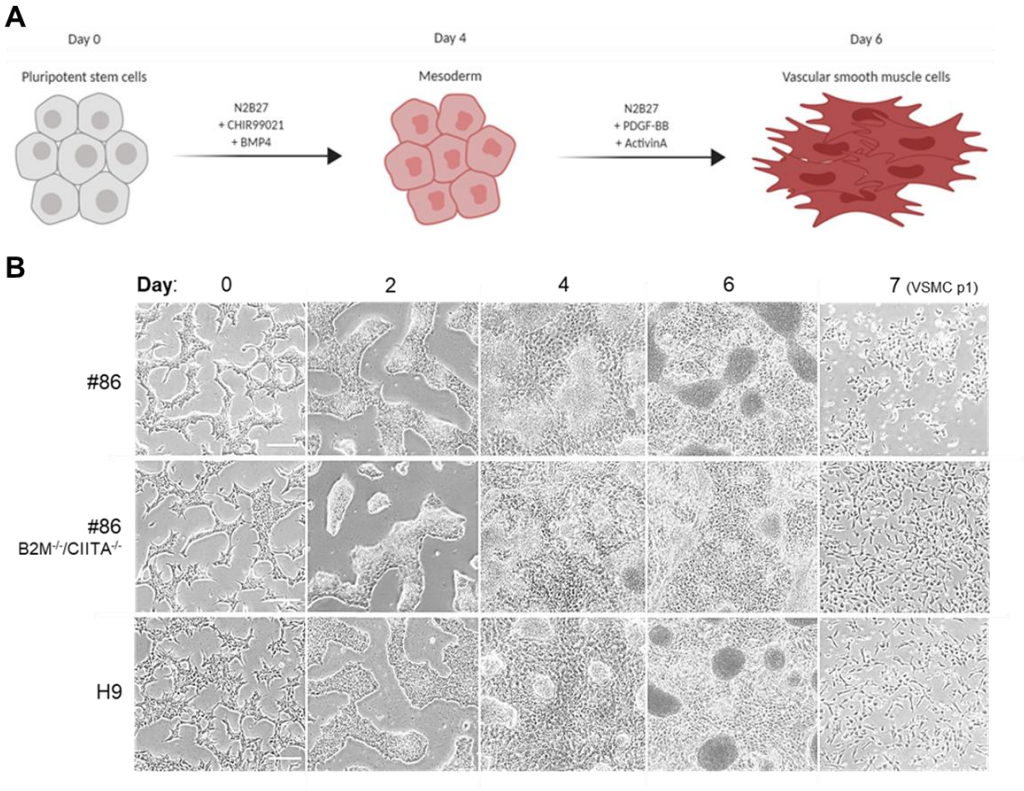


***Figure 13**: Strategy 1 for generation of VSMC by differentiating hPSCs. **A** Schematic illustration of the VSMC differentiation strategy 1 for hPSCs. (The image was created with BioRender.com.) **B** Representative brightfield images of VSMC differentiation of #86, #86 B2M$^{-/-}$/CIITA$^{-/-}$ and H9 according to strategy 1 on day 0, 2, 4, 6 and 7 after re-plating the cells. Scale bars, 200 µm.*

On day 6 of the differentiation, samples of the cells were taken and stained for CD140b (= platelet derived growth factor receptor beta, PDGFRB) which is extensively expressed in VSMCs, for flow cytometry. Figure 14A shows that around 80-95% of the WT #86 and H9 and genome-edited #86 B2M$^{-/-}$/CIITA$^{-/-}$ cells were CD140b+ at the end of the differentiation. However, an increase in CD140b expression could be observed after further culturing the cells for 4-5 days, which can be seen in Figure 14B. As the cells were split (p2), samples were stained for CD140b and used for flow cytometry. This suggests that further culture of the differentiated VSMC in SmGM-2 medium promotes VSMC-specific CD140b expression.

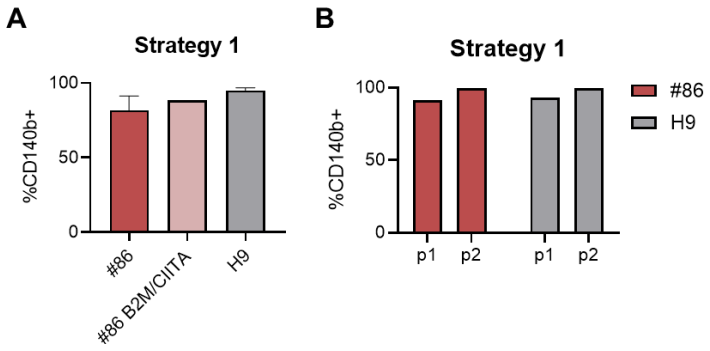


***Figure 14**: VSMC differentiation efficiency – strategy 1. **A** #86, #86 B2M$^{-/-}$/CIITA$^{-/-}$ and H9 differentiated VSMC according to strategy 1 stained for CD140b on day 6 of the differentiation (p1). n=3 independent differentiation experiments. **B** Increase of CD140b+ cells after passaging the cells from p1 to p2 measured by FACS.*

For further phenotypic characterization, immunofluorescent staining of the primary AoSMCs and the differentiated VSMC from the hPSCs lines #86, #86 B2M$^{-/-}$/CIITA$^{-/-}$ and H9 were performed. The cells were stained for F-actin, which is a key component of the cell's cytoskeleton, and the two structural proteins αSMA and SM22α, which are commonly found in VSMCs. The images in the individual channels as wells as the merged image can be seen in Figure 15. There are no obvious differences in expression patterns, and it shows that the genome-edited #86 B2M$^{-/-}$/CIITA$^{-/-}$ cells have a similar phenotype compared to the #86 WT cells.

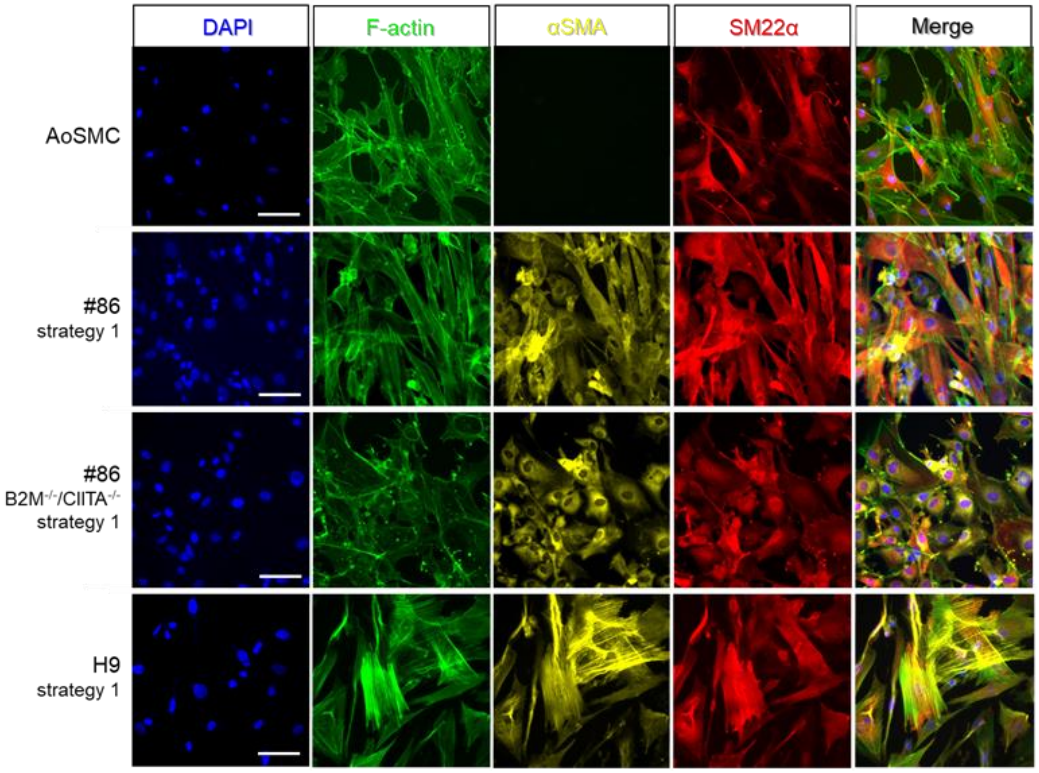


***Figure 15**: Immunofluorescent staining of AoSMCs (p8), #86, #86 B2M$^{-/-}$/CIITA$^{-/-}$ and H9 (all p2) , differentiated using strategy 1, for F-actin, αSMA and SM22α.Scale bars, 100 µm.*

Morphological changes could be observed between early and late passage #86 hPSC-derived VSMC, which are shown in Figure 17. The VSMCs were cultured in SmGM-2 medium and between p7 and p9 the cells start to change their morphology from being stretched-out and spindle-shaped to a rather enlarged and cobblestone-like shape with a lower nucleus to cytoplasm ratio. This enlarged morphology is associated with a rather synthetic phenotype and loss of contractile cellular markers (Rensen, Doevendans, & van Eys, 2007). It is known that transition from contractile to synthetic phenotype of VSMCs leads to gradual depletion of contractile filaments and establishment of a higher number of organelles involved in protein synthesis. Loss of αSMA expression, which is a contractile filament, of the late passage #86 VSMCs compared to earlier passage VSMCs can also be seen in the immunostainings in Figure 15.

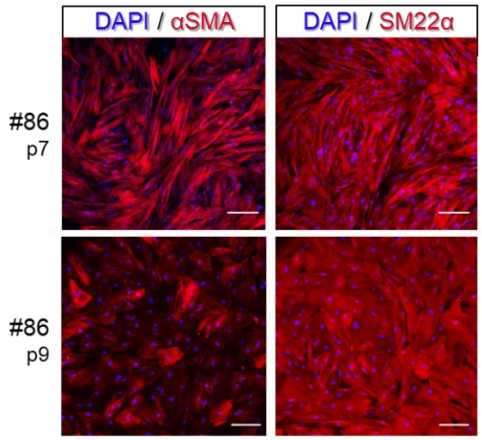


***Figure 16**: Immunofluorescence staining of early (p7) and late (p9) passage #86 hPSC-derived VSMCs (differentiation strategy 1) for αSMA and SM22α. Scale bars, 500 µm.*

### 3.2.2 VSMC Differentiation – Strategy 2

Strategy 2, previously published in Zhang et al. 2019, lasts 24 days. It also starts by inducing mesoderm by addition of CHIR9902, BMP4 as well as ActivinA for 36 h. TGF-β is added as it was shown to have a mesoderm-inducing effect (Gadue, Huber, Paddison, & Keller, 2006) for 18 h. Then the cells are pushed into the direction of VSMC progenitors using FGF, VEGF-A and Resveratrol. Lastly, there is a final 12-day maturation period where treatment with RepSox and Resveratrol should lead to a rather contractile phenotype of the VSMCs. The cells are split on day 16 and day 24 of the differentiation. The exact differentiation strategies are explained in *2.1 hPSC culture and differentiation*. A schematic illustration of the differentiation strategy 2 can be seen in Figure 17A. Strategy 2 was only performed with the WT #86 and H9 as it should just serve as a comparison of the differentiation efficiency and differences in cellular maturity in the first run. Also, here clear morphological changes can be seen in Figure 17B as the cells start to elongate and appear more spindle-shaped. Not much cellular proliferation can be observed comparing the images of day 17 and 24.

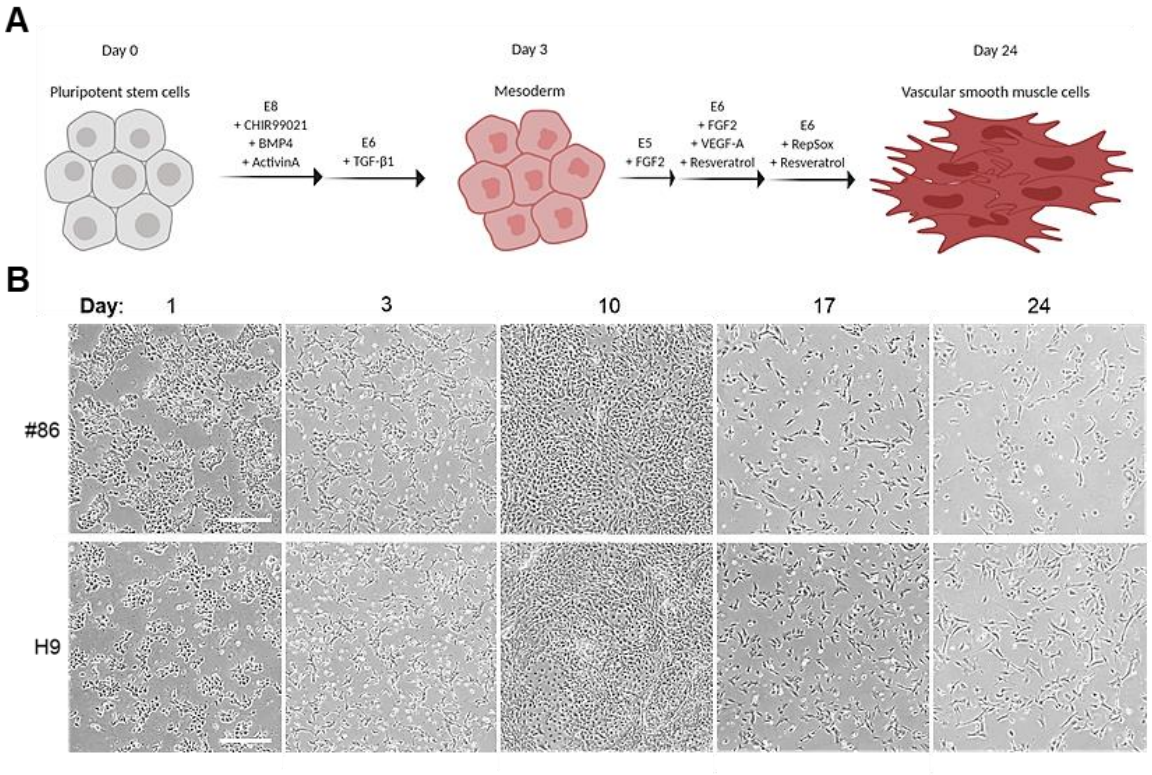


***Figure 17**: Strategy 2 for generation of VSMC by differentiating hPSCs. **A** Schematic illustration of the VSMC differentiation strategy 2 for hPSCs. (The image was created with BioRender.com.) **B** Representative brightfield image of VSMC differentiation of #86 and H9 according to strategy 2 on day 1, 3, 10, 17 and 24. Scale bars, 200 µm.*

When performing the VSMC differentiation according to strategy 2, the cells must be split on day 16 and on day 24. On both days, samples were stained for CD140b and used for FACS. Figure 18A shows the %CD140+ cells on day 16 and day 24 for VSMC differentiated from #86 and H9. A tendentious increase in CD140b expression can be seen when comparing the expression on day 16 and day 24 from the #86 and H9. For both cell lines an around 15% increase of CD140b expression can be observed. This suggests that during further eight days of maturation in the protocol of strategy 2 the cells still maturate and acquire a more VSMC-like phenotype determined by CD140b expression. However, as the error bars are relatively high for the values on day 16, the experiments would need to be repeated to achieve more significant results.

Further, smooth muscle myosin heavy chain (MYH11) and collagen type I alpha I (COL1A1) expression was measured by qPCR during the course of the VSMC differentiation according to strategy 2. MYH11 is a VSMC-specific marker for a mature contractile phenotype. COL1A1 expression is associated with a rather synthetic phenotype of VSMCs as it is a major ECM component. Figure 18B shows the relative MYH11 expression, normalized with the housekeeping gene RPLPO, of #86 and H9 VSMC-like cells on day 16 and day 24 of the differentiation. Then, the cells were cultured for eight more days in either E6R medium, which was already used during the 12-day maturation period of the differentiation protocol (day 12 until day 24) or in SmGM-2 medium, which was usually used for maintenance of the VSMC generated with the differentiation strategy 1. The bar graph shows an increase of MYH11 expression from day 16 to day 24. If further cultured in E6R medium, the cells upregulated MYH11 expression even more. However, using the SmGM-2 medium for further culture, it seems to have a downregulating effect on MYH11 expression. The #86 cell line exhibits higher MYH11 upregulation than the H9 cell line. However, both cell lines show the same tendency for upregulating MYH11 in response to culture with E6R medium, supplemented with the small molecules RepSox and Resveratrol, and downregulating MYH11 expression in response to culture with SmGM-2 medium, which contains amongst other growth factors 5% serum. As MYH11 is a marker for contractility of VSMCs, it can be concluded that usage of the E6R medium leads to maintenance or even further maturation to a contractile phenotype of the VSMCs while the SmGM-2 medium rather evokes a synthetic phenotype. These findings were also supported by observations concerning the cellular proliferation. The VSMCs cultured in E6R medium showed almost no further proliferation whilst in comparison, the VSMCs cultured in SmGM-2 medium still exhibited relatively high growth rates.

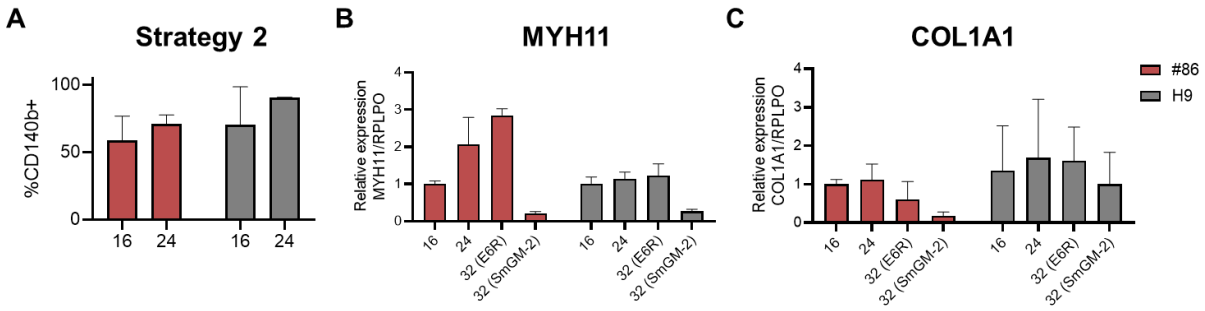


***Figure 18**: VSMC differentiation efficiency – strategy 2. **A** #86 and H9 differentiated VSMC according to strategy 2 stained for CD140b on day 16 and day 24 of the differentiation. n=2 independent differentiation experiments. **B** Relative expression of MYH11 in #86 and H9 during VSMC differentiation according to strategy 2 on day 16, 24 and after expansion in two different media (E6R and SmGM-2) on day 32. **C** Relative expression of COL1A1 in #86 and H9 during VSMC differentiation according to strategy 2 on day 16, 24 and after expansion in two different media (E6R and SmGM-2) on day 32.*

In Figure 18C, COL1A1 expression relative to the housekeeping gene RPLPO was measured. Here both cell lines, #86 and H9, show similar trends again. Interestingly, COL1A1 expression peaked on day 24 of the differentiation process and decreased after further eight days in E6R medium and reduced even more if cultured in SmGM-2 medium. Collagen type I expression was previously shown to represent a rather synthetic phenotype as it is a major ECM gene (Rensen et al., 2007; Zhang et al., 2019), which would comply with the relatively low expression on day 32 in E6R medium, where simultaneously a relatively high expression of MYH11 could be seen in Figure 18B. Unexpectedly, COL1A1 expression even further decreased if cultured in SmGM-2 medium, which was shown to have a downregulating effect on MYH11 expression (Figure 18B). If associated with a synthetic phenotype, a higher COL1A1 expression would have been expected. COL1A1 expression is also influenced by composition and organization of the ECM in which the cells are embedded and might evoke discrepancies in COL1A1 expression. However, the error bars for this experiment are relatively large. The experiment would need to be repeated to obtain more significant results.

Immunofluorescent staining of VSMC differentiated from hPSC lines #86 and H9 for F-actin, αSMA and SM22α shown in Figure 19 exhibited a similar phenotype as the

VSMC derived from hPSCs using strategy 1 (Figure 15). Both VSMC-specific markers, αSMA in yellow and SM22α in red, as well as the cytoskeletal protein F-actin are expressed in the #86 and H9 VSMCs.

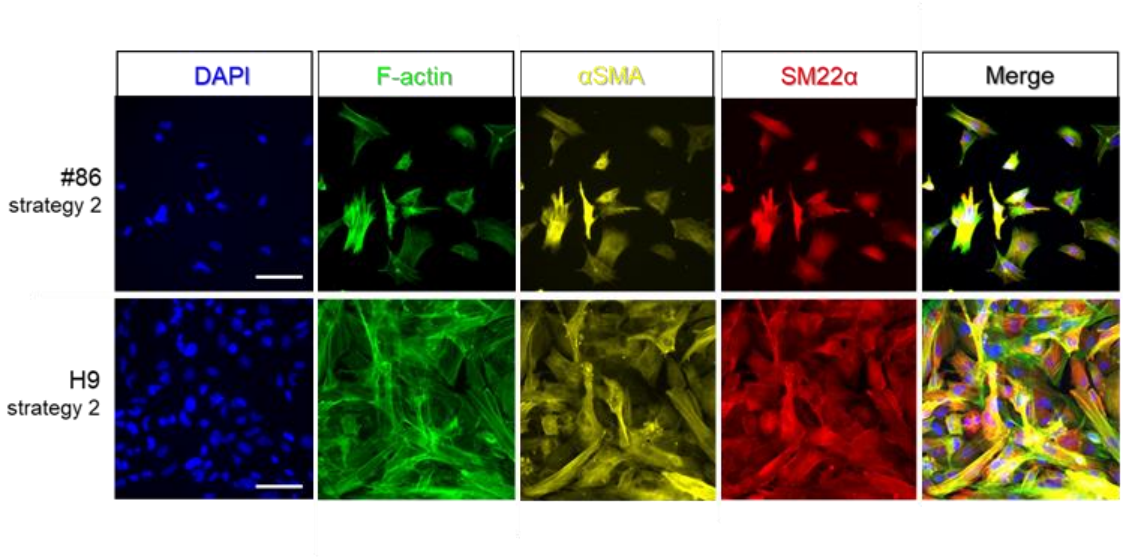


***Figure 19**: Immunofluorescent staining of #86 and H9 (both p2), differentiated using strategy 2 , for F-actin, αSMA and SM22α. Scale bars, 100 µm.*

### 3.2.3 Vascular Smooth Muscle Cell Maturation

As a synthetic phenotype of VSMCs is rather associated with vascular disease due to its migratory and proliferative behavior, a contractile phenotype would be preferred for the generation of a tissue-engineered vascular graft.

Three approaches for maturing VSMCs were tested.

#### 3.2.3.1 RepSox

The small molecule RepSox was found to inhibit contractile to synthetic phenotype switching VSMCs. It promotes the NOTCH signaling pathway and was thus found to enhance cellular contractility (Zhang et al., 2019). Figure 20 shows the MYH11 expression of 3 cell lines (AoSMCs, hPSC-derived #86 and #86 B2M$^{-/-}$/CIITA$^{-/-}$

VSMCs) after three days of treatment with 100 µM RepSox (+ RS) in SmGM-2 medium with 0.5% FBS. As a control (ctrl), cells were fed with only SmGM-2 medium with 0.5% FBS. The AoSMCs and the genome-edited #86 B2M$^{-/-}$/CIITA$^{-/-}$ VSMCs both show a more than double-fold induction of MYH11 expression after the RepSox treatment. For the WT #86 VSMCs however, there is almost no difference in MYH11 expression between the control and the RepSox-treated cells detectable.

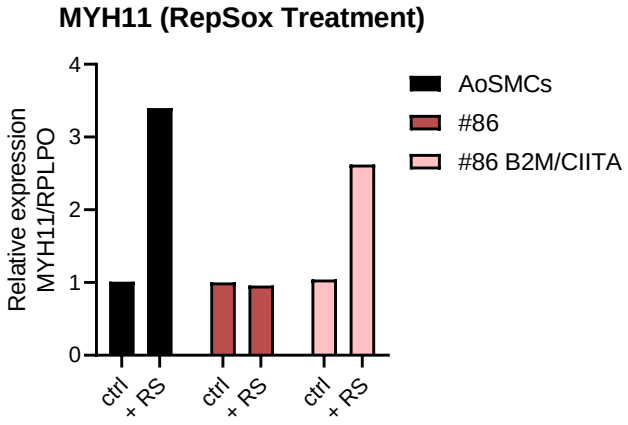


***Figure 20**: Maturation of strategy 1 derived VSMCs from primary AoSMCs and hiPSC-derived #86 and #86 B2M$^{-/-}$/CIITA$^{-/-}$ VSMCs with 100 µM RepSox-supplemented SmGM-2 medium with 0.5% FBS. Treatment was applied for 3 days and MYH11 expression was measured with RT-qPCR.*

Another approach for maturating VSMCs was to use the VSMCs generated with strategy 1 (6-day protocol) and then convert them to a rather contractile phenotype by feeding them with the maturation medium from VSMC differentiation strategy 2 (E6R medium; E6 medium supplemented with 25 µM RepSox and 25 µM Resveratrol) for 12 days. Figure 21A shows brightfield images of the 12-day maturation period of the #86 and H9 VSMCs on day 1, 6 and 12. Some morphological changes can be seen as the cells adapt a more spindle-shaped and stretched phenotype.

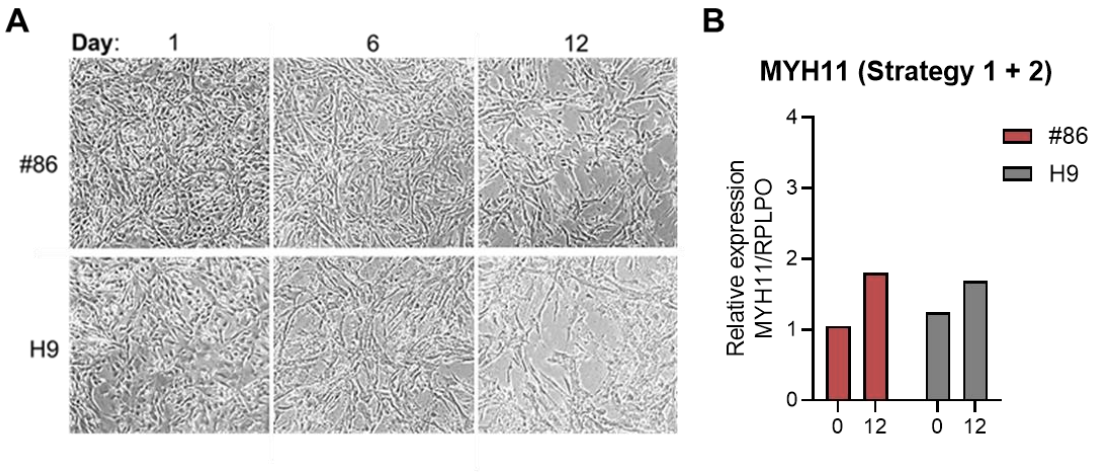


***Figure 21**: Maturation of strategy 1 derived VSMCs with final maturation medium from strategy 2. **A** 12-day maturation of #86 and H9 VSMCs using E6 medium supplemented with RepSox (25 µM) and Resveratrol (25 µM) (= strategy 1 +2). **B** Relative expression of MYH11 in #86 and H9 after VSMC differentiation using strategy 1 (day 0) and a 12-day maturation period according to strategy 2 (day 12).*

MYH11 gene expression on day 0 and day 12 of the maturation can be seen in Figure 21B. With both cell lines an increase in MYH11 expression can be detected, which indicates a switching to a rather contractile phenotype. There are some differences to the maturation performed in Figure 19 (RepSox treatment): 1) a different basal medium was used (E6 medium instead of SmGM-2 medium), 2) no serum is contained in E6R medium, 3) the concentration of RepSox is 25 µM instead of 100 µM and 4) Resveratrol is included in the E6R medium.

#### 3.2.3.2 Torin-1

Torin-1 was found to be a potent mTOR inhibitor. The small molecule simultaneously inhibits both mTOR complexes, mTORC1 and mTORC2. In 2019, Torin-1 was successfully used for maturating cardiomyocytes in a publication from the Lee laboratory at the Harvard Department of Stem Cell and Regenerative Biology (Garbern et al., 2019). This published data was the initial reason for wanting to test if Torin-1 could be also used for maturating VSMCs.

Torin-1 treatment was conducted over a time course of 9 days, as it was performed for the effective maturation of cardiomyocytes. Three different concentrations of Torin-1 were tested: 50 nM, 100 nM and 200 nM. As a control 0.02% DMSO was used. After 9 days of treatment, the used cell lines, primary AoSMCs, #86 and H9 hPSC-derived VSMC (derived using strategy 1), were used for immunofluorescent staining (Figure 22A) and detection of MYH11 expression with RT-qPCR (Figure 22B).

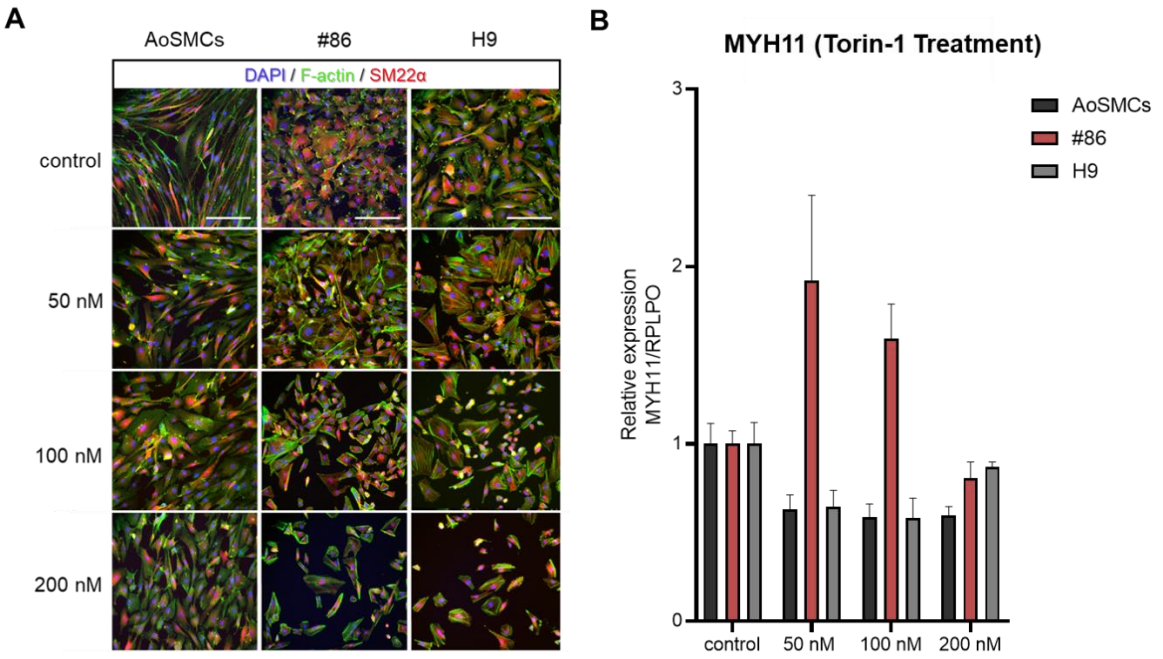


***Figure 22**: Torin-1 treatment of VSMCs. **A** Immunofluorescent staining of AoSMCs, #86 and H9 VSMCs, differentiated with strategy 1, for SM22a and F-actin after nine days of Torin-1 treatment at indicated concentrations. Scale bars, 100 µm. **B** MYH11 expression of AoSMCs, #86 and H9 VSMCs, differentiated with strategy 1, after nine days of Torin-1 treatment at indicated concentrations. 0.02% DMSO served as a control.*

The immunofluorescent staining in Figure 22A show the F-actin and SM22α expression of the AoSMCs, #86 and H9 VSMCs after nine days of Torin-1 treatment at a concentration of either 50, 100 or 200 nM. The morphology of the cells changed from a rather stretched out to a more cobblestone-like shape. Moreover, cell death could be observed at higher concentrations of Torin-1, especially with the hPSC-derived #86 and H9 VSMCs. Throughout the nine days of Torin-1 treatment the cells

maintained their SM22α expression, which indicates maintenance of the VMSC-like phenotype.

Considering the MYH11 expression, which is an indicator for VSMC contractility, an induction could be detected for the #86 VSMCs at Torin-1 concentrations of 50 nM and 100 nM. Interestingly, the two other cell lines used, AoSMCs and H9 VSMCs, did not show the same trend as they revealed a lower MYH11 expression at all tested Torin-1 concentrations. This variation could be due to differences in cellular responses to mTOR inhibition.

# 4 Discussion

## 4.1 Differentiation of hPSCs into Endothelial Cells

The differentiation of ECs from WT hiPSCs #86 and genome-edited #86 B2M$^{-/-}$/CIITA$^{-/-}$ was possible with similar differentiation efficiencies as the differentiation control hESCs H9, shown in Figure 7. Upon MACS purification 80% and upon cell sorting up to 100% pure EC populations were obtained. More cell death could be observed when sorting the cells which is probably due to high sensitivity of the differentiated ECs to elevated pressure and shear forces.

Considering the purification method, MACS is a more gentle way to purify the cells though not as high purities are obtained as with cell sorting. The possibility of cell death is however higher when sorting the cells if a too high flow rate is used. Also, for cell sorting only a smaller amount of sample can be used than for MACS as it takes too long time to sort a larger amount of sample. Thus, another approach, which would seem promising to test, would be to MACS purify the cells in the first run and then sort them in a second run with a relatively low flow rate, in case a higher purity is needed.

Another bottleneck concerning the ECs was the expansion. In order to compare different media for their ability to promote EC proliferation and maintain phenotypic stability, the differentiated ECs were cultured in either E7V medium (E6 + 100 ng/mL FGF + 50 ng/mL VEGFA), EGM-2 MV medium (EBM-2 + FGF + EGF + VEGFA + IGF + hydrocortisone + ascorbic acid + 5% FBS) or SFM (+ 20 ng/mL FGF + 50 ng/mL VEGFA). After six days of culture, all cells had died in the SFM. In both, the E7V and EGM-2 MV media, the cells maintained their phenotypic stability to the same extent measured by CD144 surface marker expression. However, the cells expanded more in the EGM-2 MV medium. This is probably due to the addition of FBS in the EGM-2 MV medium, which contains many different growth factors and hormones as well as amino acids, vitamins, trace elements and immunoglobulins and thus provokes proliferation to a greater extent than the serum-free E7V medium.

Therefore, the EGM-2 MV medium seems more suitable for the culture and expansion of primary HUVECs and hPSC-derived ECs.

The WT and genome-edited differentiated ECs were phenotypically characterized and showed similar expression of EC-specific markers, such as CD144, vWF, CD31, KDR, CD34 and CD105.

By employing functionality assays like the tube formation assay (Figure 10A), TNFα-induced ICAM-1 upregulation (Figure 10B) and the OxLDL uptake (Figure 11), it could be shown that the hPSC-derived ECs behave in a similar way as primary ECs, such as HUVECs. Also, no differences between the WT and genome-edited ECs could be detected.

Furthermore, it could be confirmed that the genome-edited #86 B2M$^{-/-}$/CIITA$^{-/-}$ are absent for HLA class I (Figure 12A). HLA class II expression is downregulated in the #86 B2M$^{-/-}$/CIITA$^{-/-}$ cells compared to the WT #86 (Figure 12B). However, it seems like there is still some slight expression, which is why confirmatory experiments would need to be made to ensure that there is no mixed population or heterozygous deletion of HLA class II. Next steps would be to perform immunoassays to further test the hypoimmunogenicity of the HLA class I and II knock-out cells. *In vitro* human peripheral blood mononuclear cells (PMBCs) or purified immune effector cells could be used, whilst *in vivo* the engineered blood vessels could be implanted into immunodeficient rats reconstituted with a functional human immune system and implant sites are examined for infiltrating macrophages or NK cells. *In vivo* vessel performance after implantation could be tested by performing histological analysis, transcriptomic profiling and biomechanical testing of the engineered blood vessels.

## 4.2 Differentiation of hPSCs into Vascular Smooth Muscle Cells

For the differentiation of hPSCs into VSMCs, two different protocols were tested. With both protocols relatively high differentiation efficiencies (80-95% for strategy 1 (Figure 14A), 75-90% for strategy 2 (Figure 18A)) could be reported, measured by

CD140b surface marker expression. To characterize the phenotype of the differentiated VSMC, marker expression of αSMA and SM22α could be confirmed by immunofluorescent staining (Figure 15 and Figure 19).

However, there was a difference between the two protocols concerning the maturity of the cells. Whilst the VSMCs seemed relatively immature on the last day of the differentiation strategy 1 (day 6), the VSMCs from the differentiation strategy 2 (day 24) had a more contractile and mature phenotype. Also, compared to the VSMCs differentiated with strategy 1, the VSMCs differentiated with strategy 2 did not proliferate as much anymore after the end of the differentiation. One reason for this might be the different media that were used for differentiating and especially maintaining the VSMCs. For strategy 1, the SmGM-2 medium was used for maintenance, which contains, next to FGF, EGF and insulin, 5% FBS. Serum was shown to induce a rather synthetic and proliferative phenotype of VSMCs (Wanjare, Kuo, & Gerecht, 2013). For strategy 2, the serum-free E6R medium lead to a rather contractile and non-proliferative state of the cells. The effect of the two different media on the MYH11 expression of the differentiated VSMCs was shown in Figure 18B. While the cells cultured in E6R medium maintained their level of MYH11 expression, the cells cultured in SmGM-2 medium had a strong reduction in MYH11 expression. This shows that the SmGM-2 medium rather provokes a proliferative and synthetic state of the VSMCs, compared to the E6R medium, which leads to a more mature and contractile phenotype.

Nevertheless, the relatively long duration of differentiation strategy 2 with 24 days is a disadvantage compared to six days with differentiation strategy 1. Another possibility to shorten the time needed to produce mature VSMCs would be to use the six-day differentiation protocol (strategy 1) and then maturate the cells. Three different approaches for the maturation of rather synthetic VSMCs were tested.

The first attempt was to add the small molecule RepSox to the SmGM-2 maintenance medium, which was shown to induce a contractile VSMC phenotype (Zhang et al., 2019). After three days of culture, an induction of MYH11 expression could be measured in 2 out of 3 cell lines (Figure 20). A reason for this could possibly be that different cell lines respond to stimuli in different ways. Maybe the WT #86

VSMCs would need more time exposed to RepSox treatment in order to adapt their phenotype and gene expression. Further repetitions of the experiment would be needed in order to make definite claims. Nonetheless, a tendency of MYH11 induction can be detected. The next step would be to test the effect of differences in concentration and exposure time of RepSox on MYH11 expression of the VSMCs.

The second approach was to combine the six-day differentiation protocol (strategy 1) with the 12-day maturation period of differentiation strategy 2 using the E6R medium, which is serum-free and contains RepSox as well. For both cell lines tested, the WT #86 and H9 differentiated VSMCs, there was an increase in MYH11 expression (Figure 21). Compared to the first maturation method, where only RepSox was added to the normal maintenance medium (SmGM-2 medium) instead of changing the basal medium as well to E6R medium, there was not as much of an increase in MYH11 expression.

Due to a recent publication where an mTOR inhibitor, Torin-1, was used to maturate cardiomyocytes (Garbern et al., 2019), its effect on VSMC maturation was to be tested. For this third maturation method, three different concentrations of Torin-1 (50, 100 and 200 nM) were used. Torin-1 was added to the medium of primary AoSMCs and hPSCs-derived #86 and H9 (strategy 1) for nine days. Whilst some cytotoxic effects could be observed at higher concentrations, especially for the hPSC-derived VSMCs, there was an induction of MYH11 expression of the #86 VSMCs at a concentration of 50 and 100 nM. The other two cell lines used, however, showed even a slight reduction in MYH11 expression at all Torin-1 concentrations tested. As mTOR inhibition is known to have the ability to activate various pathways ranging from proliferation to cell death, experimental variables such as cell type, Torin-1 concentration, stimulation time and other concurrent stimuli can influence the phenotype and gene expression of the cells (Galluzzi et al., 2012). Further repetitions of the experiment would be needed for more significant results, possibly with an alteration of treatment time or Torin-1 concentration. As the cells are to be used for the engineering of a vascular graft, another idea for solving the maturation challenge was to first seed the synthetic VSMCs onto the collagen sheets and then maturate the whole vascular graft.

In conclusion, it was possible to successfully differentiate the iPSC line #86 as well as the genome-edited #86 B2M$^{-/-}$/CIITA$^{-/-}$ into ECs and VSMCs. The phenotype of the cells was characterized by FACS and IF, using certain cell-type specific markers. The functionality of the ECs was tested and no further differences between the WT and the genome-edited cell lines could be observed in the tube formation assay, TNFα-induced ICAM-1 upregulation or the OxLDL uptake. For the maturation of the VSMCs, three different approaches were tested and compared. RepSox treatment in the first and second maturation approach showed promising results, although further experiments are needed to clarify if it is applicable to all used cell lines. Additional work needs to be done by testing if the hPSC-derived vascular wall cells have the ability to stick to the collagen sheets used for fabricating the tissue-engineered vascular grafts. Finally, the vascular graft needs to be tested *in vivo* for maintenance of phenotypic stability as well as evasion of immunological rejection.

# List of References

Conte, M. S., Bandyk, D. F., Clowes, A. W., Moneta, G. L., Seely, L., Lorenz, T. J., . . . Investigators, Prevent Iii. (2006). Results of PREVENT III: a multicenter, randomized trial of edifoligide for the prevention of vein graft failure in lower extremity bypass surgery. *J Vasc Surg, 43*(4), 742-751; discussion 751. doi:10.1016/j.jvs.2005.12.058

Dahl, S. L., Kypson, A. P., Lawson, J. H., Blum, J. L., Strader, J. T., Li, Y., . . . Niklason, L. E. (2011). Readily available tissue-engineered vascular grafts. *Sci Transl Med, 3*(68), 68ra69. doi:10.1126/scitranslmed.3001426

Di Pietro, N., Formoso, G., & Pandolfi, A. (2016). Physiology and pathophysiology of oxLDL uptake by vascular wall cells in atherosclerosis. *Vascul Pharmacol, 84*, 1-7. doi:10.1016/j.vph.2016.05.013

Fang, J., & Hirschi, K. (2019). Molecular regulation of arteriovenous endothelial cell specification. *F1000Res, 8*. doi:10.12688/f1000research.16701.1

Gadue, P., Huber, T. L., Paddison, P. J., & Keller, G. M. (2006). Wnt and TGF-beta signaling are required for the induction of an in vitro model of primitive streak formation using embryonic stem cells. *Proc Natl Acad Sci U S A, 103*(45), 16806-16811. doi:10.1073/pnas.0603916103

Galluzzi, L., Morselli, E., Kepp, O., Vitale, I., Younes, A. B., Maiuri, M. C., & Kroemer, G. (2012). Evaluation of rapamycin-induced cell death. *Methods Mol Biol, 821*, 125-169. doi:10.1007/978-1-61779-430-8_9

Garbern, J. C., Helman, A., Sereda, R., Sarikhani, M., Ahmed, A., Escalante, G. O., . . . Lee, R. T. (2019). Inhibition of mTOR Signaling Enhances Maturation of Cardiomyocytes Derived from Human Induced Pluripotent Stem Cells via p53-Induced Quiescence. *Circulation*. doi:10.1161/CIRCULATIONAHA.119.044205

Han, X., Wang, M., Duan, S., Franco, P. J., Kenty, J. H., Hedrick, P., . . . Cowan, C. A. (2019). Generation of hypoimmunogenic human pluripotent stem cells. *Proc Natl Acad Sci U S A, 116*(21), 10441-10446. doi:10.1073/pnas.1902566116

L'Heureux, N., Dusserre, N., Konig, G., Victor, B., Keire, P., Wight, T. N., . . . McAllister, T. N. (2006). Human tissue-engineered blood vessels for adult arterial revascularization. *Nat Med, 12*(3), 361-365. doi:10.1038/nm1364

L'Heureux, N., Paquet, S., Labbe, R., Germain, L., & Auger, F. A. (1998). A completely biological tissue-engineered human blood vessel. *FASEB J, 12*(1), 47-56. doi:10.1096/fasebj.12.1.47

Loh, K. M., Chen, A., Koh, P. W., Deng, T. Z., Sinha, R., Tsai, J. M., . . . Weissman, I. L. (2016). Mapping the Pairwise Choices Leading from Pluripotency to Human Bone, Heart, and Other Mesoderm Cell Types. *Cell, 166*(2), 451-467. doi:10.1016/j.cell.2016.06.011

Masternak, K., Muhlethaler-Mottet, A., Villard, J., Zufferey, M., Steimle, V., & Reith, W. (2000). CIITA is a transcriptional coactivator that is recruited to MHC class II promoters by multiple synergistic interactions with an enhanceosome complex. *Genes Dev, 14*(9), 1156-1166.

Mattapally, S., Pawlik, K. M., Fast, V. G., Zumaquero, E., Lund, F. E., Randall, T. D., . . . Zhang, J. (2018). Human Leukocyte Antigen Class I and II Knockout Human Induced Pluripotent Stem Cell-Derived Cells: Universal Donor for Cell Therapy. *J Am Heart Assoc, 7*(23), e010239. doi:10.1161/JAHA.118.010239

Mazurek, R., Dave, J. M., Chandran, R. R., Misra, A., Sheikh, A. Q., & Greif, D. M. (2017). Vascular Cells in Blood Vessel Wall Development and Disease. *Adv Pharmacol, 78*, 323-350. doi:10.1016/bs.apha.2016.08.001

Mehta, R. H., Ferguson, T. B., Lopes, R. D., Hafley, G. E., Mack, M. J., Kouchoukos, N. T., . . . Project of Ex-vivo Vein Graft Engineering via Transfection, I. V. Investigators. (2011). Saphenous vein grafts with multiple versus single distal targets in patients undergoing coronary artery bypass surgery: one-year graft failure and five-year outcomes from the Project of Ex-Vivo Vein Graft Engineering via Transfection (PREVENT) IV trial. *Circulation, 124*(3), 280-288. doi:10.1161/CIRCULATIONAHA.110.991299

National Heart, Lung and Blood Institute. (2006). Atherosclerosis. Retrieved from https://www.nhlbi.nih.gov/health-topics/atherosclerosis

Owens, G. K., Kumar, M. S., & Wamhoff, B. R. (2004). Molecular regulation of vascular smooth muscle cell differentiation in development and disease. *Physiol Rev, 84*(3), 767-801. doi:10.1152/physrev.00041.2003

Panopoulos, A. D., D'Antonio, M., Benaglio, P., Williams, R., Hashem, S. I., Schuldt, B. M., . . . Frazer, K. A. (2017). iPSCORE: A Resource of 222 iPSC Lines Enabling Functional Characterization of Genetic Variation across a Variety of Cell Types. *Stem Cell Reports, 8*(4), 1086-1100. doi:10.1016/j.stemcr.2017.03.012

Parthasarathy, S., Raghavamenon, A., Garelnabi, M. O., & Santanam, N. (2010). Oxidized low-density lipoprotein. *Methods Mol Biol, 610*, 403-417. doi:10.1007/978-1-60327-029-8_24

Patsch, C., Challet-Meylan, L., Thoma, E. C., Urich, E., Heckel, T., O'Sullivan, J. F., . . . Cowan, C. A. (2015). Generation of vascular endothelial and smooth muscle cells from human pluripotent stem cells. *Nat Cell Biol, 17*(8), 994-1003. doi:10.1038/ncb3205

Qiu, J., & Hirschi, K. K. (2019). Endothelial Cell Development and Its Application to Regenerative Medicine. *Circ Res, 125*(4), 489-501. doi:10.1161/CIRCRESAHA.119.311405

Quint, C., Kondo, Y., Manson, R. J., Lawson, J. H., Dardik, A., & Niklason, L. E. (2011). Decellularized tissue-engineered blood vessel as an arterial conduit. *Proc Natl Acad Sci U S A, 108*(22), 9214-9219. doi:10.1073/pnas.1019506108

Rajagopal, J., & Stanger, B. Z. (2016). Plasticity in the Adult: How Should the Waddington Diagram Be Applied to Regenerating Tissues? *Dev Cell, 36*(2), 133-137. doi:10.1016/j.devcel.2015.12.021

Rensen, S. S., Doevendans, P. A., & van Eys, G. J. (2007). Regulation and characteristics of vascular smooth muscle cell phenotypic diversity. *Neth Heart J, 15*(3), 100-108. doi:10.1007/bf03085963

Roh, J. D., Nelson, G. N., Brennan, M. P., Mirensky, T. L., Yi, T., Hazlett, T. F., . . . Breuer, C. K. (2008). Small-diameter biodegradable scaffolds for functional vascular tissue engineering in the mouse model. *Biomaterials, 29*(10), 1454-1463. doi:10.1016/j.biomaterials.2007.11.041

Roh, J. D., Sawh-Martinez, R., Brennan, M. P., Jay, S. M., Devine, L., Rao, D. A., . . . Breuer, C. K. (2010). Tissue-engineered vascular grafts transform into mature blood vessels via an inflammation-mediated process of vascular remodeling. *Proc Natl Acad Sci U S A, 107*(10), 4669-4674. doi:10.1073/pnas.0911465107

Syedain, Z. H., Meier, L. A., Bjork, J. W., Lee, A., & Tranquillo, R. T. (2011). Implantable arterial grafts from human fibroblasts and fibrin using a multi-graft pulsed flow-stretch bioreactor with noninvasive strength monitoring. *Biomaterials, 32*(3), 714-722. doi:10.1016/j.biomaterials.2010.09.019

Takahashi, K., & Yamanaka, S. (2006). Induction of pluripotent stem cells from mouse embryonic and adult fibroblast cultures by defined factors. *Cell, 126*(4), 663-676. doi:10.1016/j.cell.2006.07.024

Tennant, M., & McGeachie, J. K. (1990). Blood vessel structure and function: a brief update on recent advances. *Aust N Z J Surg, 60*(10), 747-753. doi:10.1111/j.1445-2197.1990.tb07468.x

Thomson, J. A., Itskovitz-Eldor, J., Shapiro, S. S., Waknitz, M. A., Swiergiel, J. J., Marshall, V. S., & Jones, J. M. (1998). Embryonic stem cell lines derived from human blastocysts. *Science, 282*(5391), 1145-1147. doi:10.1126/science.282.5391.1145

Topol, Eric. (2007). *Textbook of Cardiovascular medicine*: Lippincott Williams & Wilkins.

Waddington, C. H. (1957). *The strategy of genes*. London: Allen & Unwin.

Wang, D., Quan, Y., Yan, Q., Morales, J. E., & Wetsel, R. A. (2015). Targeted Disruption of the beta2-Microglobulin Gene Minimizes the Immunogenicity of Human Embryonic Stem Cells. *Stem Cells Transl Med, 4*(10), 1234-1245. doi:10.5966/sctm.2015-0049

Wanjare, M., Kuo, F., & Gerecht, S. (2013). Derivation and maturation of synthetic and contractile vascular smooth muscle cells from human pluripotent stem cells. *Cardiovasc Res, 97*(2), 321-330. doi:10.1093/cvr/cvs315

Wu, G., & Scholer, H. R. (2016). Lineage Segregation in the Totipotent Embryo. *Curr Top Dev Biol, 117*, 301-317. doi:10.1016/bs.ctdb.2015.10.014

Wu, W., Allen, R. A., & Wang, Y. (2012). Fast-degrading elastomer enables rapid remodeling of a cell-free synthetic graft into a neoartery. *Nat Med, 18*(7), 1148-1153. doi:10.1038/nm.2821

Zakrzewski, W., Dobrzynski, M., Szymonowicz, M., & Rybak, Z. (2019). Stem cells: past, present, and future. *Stem Cell Res Ther, 10*(1), 68. doi:10.1186/s13287-019-1165-5

Zhang, J., Chu, L. F., Hou, Z., Schwartz, M. P., Hacker, T., Vickerman, V., . . . Thomson, J. A. (2017). Functional characterization of human pluripotent stem cell-derived arterial endothelial cells. *Proc Natl Acad Sci U S A, 114*(30), E6072-E6078. doi:10.1073/pnas.1702295114

Zhang, J., McIntosh, B. E., Wang, B., Brown, M. E., Probasco, M. D., Webster, S., . . . Thomson, J. A. (2019). A Human Pluripotent Stem Cell-Based Screen for Smooth Muscle Cell Differentiation and Maturation Identifies Inhibitors of Intimal Hyperplasia. *Stem Cell Reports, 12*(6), 1269-1281. doi:10.1016/j.stemcr.2019.04.013

# ANNEX

***Table 1**: Antibodies – Immunofluorescence Staining*

| Antigen | Host | Dilution | Vendor | Catalog Number |
|---|---|---|---|---|
| Primary Antibodies | | | | |
| aSMA | mouse | 1/250 | Dako | M0851 |
| SM22a (transgelin) | rabbit | 1/200 | Abcam | ab14106 |
| CD144 (VE-cadherin) | goat | 1/100 | R&D Systems | AF938 |
| vWF | rabbit | 1/400 | Dako | A0082 |
| Alexa Fluor 568 Phalloidin | | 5/200 | Invitrogen | A12380 |
| Alexa Fluor 647 Phalloidin | | 5/200 | Invitrogen | A22287 |
| DAPI | | 1/10000 | Sigma | D9542-5MG |
| Secondary Antibodies | | | | |
| anti-mouse IgG Alexa Fluor 555 | donkey | 1/500 | Life technologies | A31570 |
| anti-rabbit IgG Alexa Fluor 546 | donkey | 1/500 | Life technologies | A10040 |
| anti-goat IgG Alexa Fluor 555 | donkey | 1/500 | Life technologies | A21432 |
| anti-rabbit IgG Alexa Fluor 488 | donkey | 1/500 | Life technologies | A21206 |
| anti-mouse IgM Alexa Fluor 488 | goat | 1/500 | Life technologies | A21042 |
| anti-rabbit IgG Alexa Fluor 647 | donkey | 1/500 | Life technologies | A31573 |

***Table 2**: Antibodies – Flow Cytometry*

| Antigen | Colour | Dilution | Vendor | Catalog Number |
|---|---|---|---|---|
| Endothelial Cells | | | | |
| CD31 (PECAM-1) | APC | 1/100 | BioLegend | 303115 |
| CD34 | PE | 1/100 | Miltenyi Biotec | 130-098-140 |
| CD45 | APC | 1/100 | BioLegend | 368511 |
| CD54 (ICAM-1) | PE | 1/100 | Miltenyi Biotec | 130-107-457 |
| CD105 | PE | 1/100 | BioLegend | 323205 |
| CD144 (VE-cadherin) | FITC | 1/100 | BD Pharmingen | 560874 |
| CD144 (VE-cadherin) | PE | 1/100 | BD Pharmingen | 560410 |
| CD309 (KDR) | PE | 1/100 | Miltenyi Biotec | 130-098-905 |
| Vascular Smooth Muscle Cells | | | | |
| CD140b | PE | 1/100 | BD Pharmingen | 558821 |
| HLA Class I & II | | | | |
| W6/32 | PE | 1/100 | BioLegend | 311406 |
| HLA-DR | APC | 1/100 | Invitrogen | MA1-10347 |

***Table 3**: TaqMan Probes - qPCR*

| TaqMan Assay | Species | Vendor | Catalog Number |
|---|---|---|---|
| MYH11 | Homo sapiens | Thermo Fisher Scientific | Hs00224610_m1 |
| COL1A1 | Homo sapiens | Thermo Fisher Scientific | Hs00164004_m1 |
| RPLPO | Homo sapiens | Thermo Fisher Scientific | Hs00420895_gH |